Climate Related Changes to Flood Regimes Show an Increasing Rainfall Influence

Donald H. Burn[a*] ORCID: 0000-0001-7917-6380

Paul H. Whitfield[b,c,d] ORCID: 0000-0001-6937-9459

[a]Department of Civil and Environmental Engineering, University of Waterloo, 200 University Avenue W., Waterloo, ON Canada, N2L 3G1, donburn369@gmail.com

[b]Centre for Hydrology, University of Saskatchewan, Saskatoon, SK, paul.h.whitfield@gmail.com

[c]Department of Earth Sciences, Simon Fraser University, Burnaby, BC

[d]Environment and Climate Change Canada, Vancouver, BC

[*]Corresponding author.

Abstract

Climate change can result in changes to floods and flood regimes, but the relationship between floods and climate change is complex and poorly understood. The flood regime influences the nature, severity, and timing of flood events for any watershed. Flood regimes should be viewed as a continuum with completely nival (snowmelt-driven) watersheds at one end of the continuum and purely pluvial (rainfall-driven) watersheds at the other. Flood regimes are important for the operation of flood defenses and to better understand how changes in the flood regime can affect the magnitude of flood events. Data from 46 long term streamflow gauging stations from reference hydrologic networks (RHNs) in Canada (23) and the US (23), are examined to detect changes that have occurred, or are continuing to occur, in flood regimes from watersheds responding only to climate variations and changes. Peaks over Threshold (POT) flood events are used to investigate changes in the timing of flood events. Seasonality measures, using circular statistics, illustrate changes in the nature of the flood regime based on changes in the timing and regularity of flood threshold exceedences. A nival fraction is determined for each watershed and for each year based on a clustering of the flood events into two groups, representing nival and pluvial events. Changes to the flood regime over time, and based on annual temperature, are determined from logistic regression of the number of nival and pluvial events for each year. While strongly nival watersheds show no changes, roughly 15% of the stations exhibit significant changes that represent shifts towards the pluvial end of the flood regime continuum, which has implications for design flood estimation and the operation of flood control infrastructure.

Keywords: floods; shifting flood regimes; climate change; flood frequency analysis

1.0 Introduction

In flood frequency analysis it is assumed that the flood series arises from a single distribution and the flood events are statistically independent. This is not the case where there are multiple flood generating processes (Waylen & Woo, 1982) or changes in the flood regime occur over time with either climate change or observed shifts in the climate system modes (Franks, 2002). Changes to the flood regime can result in a nonstationary flood series and/or a mixture of flood generation processes, both of which require special consideration in flood frequency analysis used to estimate design flood values. Flood frequency methods are predominantly based on event magnitude; the method presented here uses circular statistics to separate flood events based upon their day of occurrence as a surrogate for flood generating process. In cold regions, nival processes, such as snowmelt, dominate flood occurrence and timing; an indicator is introduced to identify basins that may be more sensitive to change.

Flood regime shifts resulting from global warming occur because a warmer atmosphere has an increased capacity to redistribute water suggesting an increase in precipitation and heavy rains. The risk of flooding increases with more intense precipitation (Trenberth, 2005). In cold regions, a warmer climate is expected to shift the form of precipitation towards rainfall and away from snow, and as snow melts earlier in the year in continental and cold regions, there is an increased risk of flooding in spring (Trenberth, 2005). While there is evidence indicating increasing intensification of the water cycle, flood data do not show widespread increasing trends in floods (Huntington, 2006; Sharma *et al*., 2018). Projections of floods in future climates involve complex issues that defy generalizations (Whitfield, 2012). Changes in flood attributes may result from changes occurring in the atmosphere, the catchment landscape, and river modifications such as reservoirs (Bertola *et al*., 2019). The complexity of flood generating mechanisms in space and time demands careful assessment that needs to include considering the flood regime as a continuum from nival to pluvial with atmospheric changes, particularly warming, shifting many rivers towards the pluvial end of the continuum (Burn & Whitfield, 2018).

There have been numerous studies examining the effects of climate change on floods in cold regions. Where snow accumulation and melt are important in a catchment during the flood period, the anticipated changes in flood seasonality are most pronounced (Köplin *et al*., 2014; Vormoor *et al*., 2016) but changes in summer precipitation also affect the timing and annual regularity of floods. This results in both the magnitude and frequency of events changing as rainfall becomes a more important flood generating process and the contribution of snowmelt to flooding decreases. Climate change will alter flood hazard by changing flood magnitudes and frequency, although the nature of these changes varies by country and region. In North America, snowmelt floods are occurring earlier and decreasing in magnitude (Cunderlik & Ouarda, 2009); however, increases in fall flood event magnitudes (Cunderlik & Ouarda, 2009) and frequency (Whitfield & Shook, 2020) have been observed. Projections also show that snowpacks will be reduced leading to earlier peak flows and lower runoff volumes (Hamlet & Lettenmaier, 1999). In the United States, there is little evidence of changes in the magnitude of floods but evidence of increasing frequency (Mallakpour & Villarini, 2015) due to increasing temperature and changes in seasonal rainfall. While trends in magnitude, frequency, duration and volume of frequent floods show large changes, few are statistically significant (Archfield *et al*., 2016); the lack of spatial patterns of the trends indicates a complex fragmented pattern of changes in floods making generalizations difficult. Shifts in the time of occurrence may be indicative of an increasing frequency of events or of changes in flood generating processes.

Floods in other cold regions have decreased or are unchanged, while increased precipitation has increased floods in others. Changes in timing have been observed in Europe, but no consistent large-scale signal in magnitudes has been observed (Blöschl *et al*., 2017). Mediero *et al*. (2014) identified decreasing trends in flood magnitude and frequency in northwest Spain with floods occurring later. Merz *et al*. (2018) demonstrate spatial coherence amongst floods at 68 gauges in Germany with flood rich and flood poor periods that are spatially coherent. Similarly, changes in annual maximum flows

oscillated between wet and dry periods but show no trends over the past 100 years in Sweden (Arheimer & Lindström, 2015), but there is an increased importance of rain in flood generation in the south with more frequent rain driven floods. In Finland, the impacts of climate change on floods are not uniform due to regional differences in climate and geography (Veijalainen *et al*., 2010); floods in snowmelt flood areas have decreased or are unchanged, while increased precipitation has increased floods in other areas. Changes in floods related to climate change are not consistent across France (Lang *et al*., 2006; Renard *et al*., 2008) but peaks have increased in the northeast, and peaks decreased and were earlier in mountainous regions. In Switzerland, the magnitudes of floods are expected to increase due to changes in both flood generating processes and extreme precipitation (Köplin *et al*., 2014). Hanus *et al*. (2021) modelled future changes in magnitude and timing of annual extreme flows in six alpine catchments in Austria suggesting earlier annual maxima by 9 to 31 days and a widening of the period for potential flooding.

In cold regions of Asia, there has been a downward trend in floods that is attributable to climate and human activities (Liu *et al*., 2017). In cold arid regions of China, floods increased on annual and seasonal time scales after the 1980's following an increase in temperature and predominantly due to rainstorms and temperature induced melting of glaciers and snowpack (Zhang *et al*., 2016). In coastal areas of China, the pattern of changes in extreme precipitation and floods were similar (Zhang *et al*., 2017). While the present focus is on the timing of floods in cold regions, in other regions shifts in flood generating process have occurred. Ganguli *et al*. (2020) report many sites show changes in the timing of floods, and a mix of nonsignificant trends in the pluvial upper Mahanadi basin (India) with increases in magnitude being pronounced in POT analysis along with a decrease in monsoonal maxima peak discharges.

Warming will also affect other aspects of the water cycle beyond precipitation including evaporation, water storage as snow and groundwater, but also snowmelt, ice cover and breakup and glacial melt. Ice-

jam floods in unregulated rivers in Canada are occurring earlier (Rokaya *et al*. 2018); however, the magnitude of these events is decreasing in the north and increasing in the south. This makes local effects very important in understanding future floods (Whitfield, 2012).

Climate variability, through climate change or climate modes (atmosphere-ocean oscillations) are globally and regionally pertinent to flooding. Diverse regions of the world exhibit synchronous changes in flood attributes related to global climatic conditions (Burn & Arnell, 1993). This synchrony may be attributable to changes in modes of the climate system. The modes, also referred to as teleconnections and climate modes, may drive interannual and interdecadal variability of flood magnitude and frequency (Hodgkins et al., 2017; Kundzewicz *et al*., 2019). The nonstationary patterns of floods in relation to climate change and with low frequency climate modes are not well understood (Jain & Lall, 2000). The role of teleconnections in relation to shifts in the time of flood occurrence is also assessed.

As expected for an increased prevalence of rainfall and a decreased prevalence of snowmelt contributions, an increase in the number of flood events exceeding a threshold and a decrease in magnitude of the exceedences were observed based on all flood regimes for 23 long record reference sites in Canada (Burn *et al*., 2016; Burn & Whitfield, 2016). These changes are more commonly detected in the mixed portions of the continuum than in the most pluvial and nival extremes (Burn & Whitfield, 2017). These shifts in generating processes cannot be detected from studies of event magnitude alone. The present research explores a larger set (46) of long record streamflow data (~80 years) from Reference Hydrologic Networks (RHNs) in Canada and the northern Unites States for changes in the cold region flood regime. Specifically, the nival fraction of the flood events for a station is used to indicate the sensitivity to change and these changes are related to potential causative factors. This work thus directly tests for changes in flood generating mechanisms rather than examining changes in flood attributes, such as the number of over threshold events or the magnitude of these events. Since flood regime is viewed as a continuum from fully nival sites to fully pluvial sites, the novel methodology uses

clustering of day of event occurrence using circular methods to separate the flood processes between nival snowmelt events and pluvial rainfall driven events. This work contributes to a greater understanding of the changes occurring in flood events in cold regions and explores the implications of these process shifts for the estimation of design floods.

2.0 Methods

2.1 Data Used

Streamflow records for 46 reference sites from the northern portion of the mid-latitudes of North America are used to examine flood regime changes over time, with changes in annual temperature, and with shifts between climate modes. All stations are part of an RHN with 23 stations from the Canadian Reference Hydrometric Basin Network (RHBN) (Brimley *et al*., 1999) and 23 sites from the U.S. Geological Survey (USGS) Hydro-Climatic Data Network (HCDN) (Lins, 2012). Choosing sites from an RHN ensures that the data are of good quality and are at most minimally impacted by regulation, diversions, or land use change. Sites that are part of an RHN have been specifically selected to evaluate the impacts of climate change on streamflow characteristics (Whitfield *et al*., 2012). The sites selected have data available for the 80-year period from 1938 to 2017. Table 1 provides a summary of the characteristics of the stations used in this analysis including the station number from the Water Survey of Canada (Canadian sites) or the USGS (US stations) as well as the station name and drainage area. Each station is assigned a site number, as shown in Table 1; the site number is also displayed on Figure 1, which shows the location of the stations. Sites 1 to 23 are from Canada and sites 24 to 46 are from the United States.

[Table 1 near here]

[Figure 1 near here]

The spatial coverage of sites in the study area is sparse, especially for the Canadian portion. The sparse coverage is a direct consequence of the criteria used in selecting sites to include in the analysis. First, only stations with at least 80 years of record were selected to ensure that long term tendencies are identified in the data records as opposed to short term fluctuations. Second, all stations selected were part of an RHN, which ensures that the data records are of good quality and are at most minimally affected by regulation or land use changes; hence changes identified can be attributed to climate factors. There are, unfortunately, comparatively few sites with long term data records that also reflect totally pristine conditions.

Peaks over threshold (POT) data were extract for all sites using the graphical approach described in Burn *et al*. (2016). The POT extraction approach follows recommendations by Lang *et al*. (1999) to ensure independence of over threshold events. POT flood data were selected in this work, rather than only annual maximum flood events, to provide a more complete characterization of the flood events for a station by including all independent events above a prescribed threshold. POT data generally result in more flood events than for annual maximum data, with the potential for multiple events in a year as well as no events in years where the maximum event for the year does not exceed the threshold. Pan *et al*. (2022) provide a recent review of the literature on POT flood data indicating the superiority of POT data in comparison with annual maximum flood data, particularly in the context of flood frequency analysis.

2.2 Methodology

Multiple measures of changes in the flood regime for a watershed are considered based on changes in the nival fraction of flood events for a station. Nival fraction is the focus of the analysis since this is an understudied aspect of flood response particularly in the context of flood regime as a continuum. It is recognized that flood regimes are not completely characterized by the nival fraction of flood events.

Changes in the nival fraction between different subsets of the data record are first examined. A more formal measure of the statistical significance of changes in the nival fraction is estimated using logistic regression. Details on each element of the methodology are provided below.

In cold regions, the timing of flood events and the flood regime of a watershed are strongly interlinked; hence, seasonality measures for flood timing, defined using circular statistics (Pewsey *et al*., 2014), form the starting point for the methodology. Seasonality measures allow each station to be plotted on a polar plot where the mean flood date plots as an angle measured clockwise relative to 1 January; January 1 plots at the "six o'clock" position. The regularity of the flood events plots as the distance from the center of the plot. Flood regularity can vary from 0 to 1 with higher values indicating less spread in the timing of the flood events such that the regularity is 1 if every flood event occurs on the same day in each year. Seasonality measures, calculated using circular statistics, are used herein to display the results and are also a part of the process used to partition the flood events for a station into nival and pluvial events. Seasonality measures were calculated using the R package "circular" (Agostinelli & Lund, 2017).

The nival fraction for a station is determined by first clustering the flood events using circular clustering; clustering of seasonal events is described in Whitfield (2018). Clustering of the flood events provides a data-driven approach to identifying nival and pluvial events in the data record. The over threshold events were clustered based on the date of the maximum flow in an event. The date of the maximum flow during an over threshold event was converted to a day of the year (i.e., 1 – 365) and this was then converted to an angle using:

$$\theta_i = doy_i \frac{2\pi}{lenyr} \quad (1)$$

where θ_i is the angle (in radians) for event *i, doy*$_i$ is the day of the year for event *i* and *lenyr* is the length of the year in days (365 or 366). The x- and y-coordinates for the event are then found from:

$$x_i = -\sin(\theta_i) \quad (2)$$

$$y_i = -\cos(\theta_i) \quad (3)$$

These x- and y-coordinates provide the positions of the POT events on the unit circle. For each site, the points defined by a matrix of these x- and y-coordinates were separated into 2 clusters using partitioning around mediods (pam), a more robust version of k-means clustering (Reynolds *et al.*, 2006), with Euclidean distance as the dissimilarity measure. The pam algorithm was implemented using the R package "cluster" (Maechler *et al*., 2019).

The clustering of the events into nival and pluvial events for each station yields a vector giving the number of nival events for each year and a vector giving the number of pluvial events for each year. The nival fraction for a station is then calculated as the number of nival events divided by the total number of events for the station. It should be noted that in this work the nival events can include both snowmelt events and rain-on-snow events. The nival fraction for each station is displayed and changes in the nival fraction for different subsets of the data record are determined. The data were divided into subsets based on time (years) giving early, mid and late periods, with lengths of 27, 26 and 27 years, respectively. Changes in the nival fraction between early and mid, early and late, and mid and late periods are then determined as a form of exploratory data analysis that allows a visualization of the types of changes that are occurring between these periods. Choosing a different number of periods can alter these results. Hence, this analysis is a qualitative exploratory analysis that motivates the quantitative analysis of logistic regression.

A more formal measure of changes in the nival fraction is obtained using logistic regression (Frei & Schär, 2001). Logistic regression is used when the independent variable is binary (in the present case, either a nival event or a pluvial event – arbitrarily, nival events are a 1 and pluvial events are a 0). The input for the independent variable is the counts of nival and pluvial events for each year and the model

predicts the probability of a nival event as a function of the predictor variable. The fit of the model to the data allows the significance of any change in the nival fraction with changes in the predictor variable to be determined. For a full description of logistic-regression see Agresti (2013). Logistic regression analysis was conducted using "glm" in the "stats" R package (R Core Team, 2021).

The impacts of climate change on floods are complex and thus any selected predictor, or explanatory, variable is a surrogate for the complex array of impacts of climate change on flood events. The first predictor variable in the logistic regression analysis is the year, providing a temporal analysis. The temporal analysis is directly analogous to trend analysis of a continuous flood variable, such as flood magnitude. The second predictor variable used was annual temperature in an attempt to provide a more direct linkage between warming conditions and flood impacts. Annual temperature data were obtained using climateNA v7.10 to extract the data from 1930 to 2020 for the locations of each of the 46 sites. ClimateNA (www.climateNA.ca) is described in Wang *et al.* (2012, 2016). The final predictor variables were one of four climate indices, where values for each climate index are determined for each year. Climate modes carry the signal of low-frequency variations in the atmosphere that modify precipitation and flood potential at a local scale (Sankarasubramanian & Lall, 2003). The variability of climate modes has been widely reported in the literature and recently reviewed by Kundzewicz *et al*. (2019); each of these modes affects floods in different regions and with different effects. The climate indices used herein are the Atlantic Multidecadal Oscillation (AMO), the North Atlantic Oscillation (NAO), the Pacific Decadal Oscillation (PDO) and the Southern Oscillation Index (SOI). These climate indices were selected since they have been reported to have impacts on streamflow at locations within the study area. For each climate index, annual values are used for the current year and for the previous year, since some climate indices have been noted to have a lagged impact on flooding, resulting in eight analyses in total. While the primary focus is on changes in flood regime with time, annual temperature is also included to evaluate the relative predictive capability of annual temperature relative to time.

Additionally, there are two reasons for considering teleconnections with dominant climate indices. First, if both a trend over time and a trend in a climate index over time are detected, the time trends may be due to the trend in the index, which is common for long persistent teleconnections, such as AMO and PDO. Second, there are cases in the literature where floods and local climate have been linked to phases of climate indices, particularly SOI and NAO, and there is interest in how the present results compare.

3.0 Results

The circular clustering approach was used to identify two clusters for each site, consisting of nival and pluvial events, respectively. There are three sites that contain only nival events (sites 20, 36, and 37) and three sites that contain only pluvial events (sites 22, 39, and 46); these sites were considered to have only one cluster. The remaining 40 sites have varying mixes of nival and pluvial events with nival fractions ranging from 0.97 (site 19) to 0.17 (site 40). For site 29, the clustering revealed three evident clusters. Three clusters were extracted for this site and clusters 1 and 2 were combined resulting in two clusters that were treated the same as was done for the other sites. Figure 2 provides example polar plots of the POT events for four sites with the sites displayed having decreasing nival fractions from Figure 2a to 2d. Also shown on the polar plots in Figure 2 is a kernel density estimate for the circular distribution of the timing of flood events, calculated using the R package "circular" (Agostinelli & Lund, 2017). The circular density is provided to validate the clustering results. The clustering of flood events should group together portions of the unit circle with high density estimates and the dividing points between clusters should correspond to density values close to zero.

[Figure 2 near here]

Figure 3 is a polar plot showing the mean timing and regularity of flood events for each of the 46 sites. The nival fraction for each site is indicated by the colour inside the symbol. Strongly nival stations, such as sites 19, 20, 36, and 37, are highly regular (~1.0), have a high nival fraction (~1.00), and have a mean flood occurrence in June. Pluvial stations, such as sites 22, 39, 40, and 46, have low regularity (~0.5), a low nival fraction (< 0.20), and have a mean flood occurrence in November to January. Mixed stations experience a combination of nival and pluvial events with the nival fraction determined by whether the dominant number of events is nival (e.g., sites 13, 14, and 17) or pluvial (e.g., sites 3, 4, 5, 6, and 7). Noteworthy from Figure 3 is the general decrease in nival fraction when moving from the upper left of the polar plot to the lower right. The histogram in Figure 3 shows the number of sites for different values of nival fraction.

[Figure 3 near here]

To qualitatively investigate changes in the nival fraction at each site, the 80-year data record was divided into three approximately 27-year segments defined as the early, mid and late sections of the data record. The nival fraction was calculated for each segment for each site and the change in nival fraction between each segment was calculated by subtracting the nival fraction for the earlier segment from the nival fraction for the later segment such that positive nival fraction changes indicate an increased number of nival events in the more recent period. Figure 4 displays changes in the nival fraction for the sites. Changes from the early to the mid segment, early to late segment and mid to late segment are shown in Figures 4a to 4c, respectively. Neither the strongly nival sites nor the strongly pluvial sites show differences between the time periods, while the mixed sites show a predominance of negative changes (fewer nival events in the more recent segment). Comparison of the three plots shows that the changes in nival fraction are not uniform over time with the early segment corresponding to the most nival events. There are also notable differences in the changes in nival fraction for specific sites between the data segments, as illustrated in Figure 4d, which summarizes the nival fraction changes for

each site. Note that the sites are displayed in Figure 4d with nival fraction decreasing from top to bottom. Site 41 shows a modest decrease in nival fraction from the early to the mid segment but larger decreases in nival fraction from the early to the late and from the mid to late segments. Conversely, site 23 shows a large decrease from early to mid and also from early to late but a more modest change from mid to late. There are also sites for which the sign of the change in nival fraction is different for different segment comparisons. An example is site 9 that has a large decrease in nival fraction from the early to the mid segment, little change from early to late and an increase from mid to late. A different sign of nival fraction change for different segment comparisons is also apparent for other sites (see Figure 4d) with sites 2, 27, 32 and 34 all indicating a later onset of nival fraction decrease.

[Figure 4 near here]

Logistic regression was used to provide a more quantitative assessment of the change characteristics of the nival fraction for each site that complements the results from Figure 4 while alleviating the ambiguity that results from conflicting nival fraction change outcomes for different data segments, as noted above. Example plots of the logistic regression results are in Figure 5, which shows results for the same four sites displayed in Figure 2; plots for all sites are in Figure S1 in the Supplemental Material.

The logistic regression plots show the POT events as gray circles stacked either at nival event probability of 1.0 (nival events) or 0.0 (pluvial events) and the line of the logistic regression, which is colour coded to indicate the significance of the change in the nival fraction (solid red $p \leq 0.05$, dashed red $0.05 < p \leq 0.10$, gray $p > 0.10$). The largest POT event from each year is also shown in the form of rug plots at the top (nival events – in blue) or at the bottom (pluvial events – in red) of each plot. The series of the largest POT event from each year is not necessarily the same as the traditional annual maximum series since some annual maximum events may not exceed the threshold for the POT data; hence the series of the largest POT event from each year may be a subset of the annual maximum series.

315 [Figure 5 near here]

316 The example plots show a site with a significant decreasing change at the 5% significance level (Figure
317 5a), a decreasing change that is significant at the 10% level (Figure 5d) and sites with insignificant
318 increasing and decreasing changes (Figures 5b and 5c, respectively). Site 14 shown in Figure 5a has a
319 large nival fraction with pluvial events first occurring in the late 1960s and becoming more frequent in
320 the latter part of the record. Notice that for this site, there are two years for which the largest POT
321 event is a pluvial event as indicated by the rug plot on the lower axis (red tick marks). In contrast to site
322 14, site 40 (Figure 5d) has a much smaller nival fraction and the change in the nival fraction over time
323 seems to be driven by the increased frequency of pluvial events with the frequency of nival events being
324 low but somewhat consistent throughout the period of record. Sites 2 and 4, shown in Figures 5b and
325 5c, respectively, have a mixture of nival and pluvial events. Both sites have non-significant changes in
326 the nival fraction with time based on logistic regression with a decreasing tendency for site 4 and an
327 increasing tendency for site 2. The latter outcome is consistent with the results displayed in Figure 4d.

328 Figure 6 is a map showing the change in nival fraction for each of the sites. Shown are the sites with a
329 significant decreasing change in nival fraction at the 5 or 10% significance level, sites that have a non-
330 significant increasing or decreasing change as well as the six sites that exhibit no change. Note that the
331 six sites with no change are those with all nival or all pluvial events and hence the nival fraction is always
332 1 or always 0, respectively, for all values of the explanatory variable. For display purposes, the symbols
333 only show the greatest level of significance such that the sites shown as having a decreasing change at
334 the 10% significance level do not include the sites with a decreasing change at the 5% significance level.
335 This convention is followed elsewhere in the paper as well. Note that there are no sites with significant
336 increasing changes. There is a grouping of sites with significant decreasing changes in the east/central
337 part of the study area as well as a further two sites on the west coast. The sites with a non-significant
338 increasing change are all located in the eastern part of the study area and all are in Canada. Figure 7

339 provides a similar breakdown of the change status for each site on a plot of nival event fraction versus
340 the fraction of nival maximum POT events. Figure 7 uses the same symbols and colours that are used in
341 Figure 6 to denote change status. The three sites that have only nival events plot in the upper right
342 corner of Figure 7 at the point (1.0, 1.0) and the three sites with only pluvial events plot in the lower left
343 corner at the point (0.0, 0.0). For clarity, the three points in each of these corners are separated slightly
344 to emphasize that there are three points in each corner, each with the coordinates of (1.0, 1.0) or (0.0,
345 0.0) for nival and pluvial sites, respectively. The remaining 40 sites have a mix of nival and pluvial POT
346 events and all have a fraction of nival maximum POT events that is less than one and greater than zero.
347 Hence, each of these sites has at least one year with a nival maximum POT event and at least one year
348 with a pluvial maximum POT event, as can also be seen from the rug plots of the logistic regression
349 results in Figure S1 in the Supplemental Material. This suggests that the changes that are occurring in
350 the mix of nival and pluvial events is not limited to events that are close to the POT extraction threshold
351 but rather that at least some of these changes involve substantial events. Many of the sites with a high
352 nival fraction have a very small number of years for which the maximum POT event for the year is pluvial
353 and hence these sites plot close to 1.0 on the y-axis. Figure 7 reveals that most of the sites with
354 significant changes in nival fraction are sites with a high nival fraction; all but one of the significant
355 changes correspond to sites with a nival fraction in excess of around 0.7. The exception is site 40, which
356 has the lowest non-zero nival fraction. The five sites with non-significant increases in nival fraction show
357 no particular pattern on Figure 7.

358 [Figure 6 and Figure 7 near here]

359 Table 2 summarizes the results from logistic regression when applied on a temporal basis, based on
360 annual temperature, and based on each of the four climate indices as well as climate indices lagged by
361 one year. Note that the categories in Table 2 are non-overlapping and include all possible outcomes;
362 hence, the sum of the entries in each column must equal the number of sites, which is 46. Table 2

363 reveals that the number of significant changes are very similar for the temporal analysis and for the
364 analysis based on annual temperature, with the sole difference being one increasing significant change
365 (5% significance level) for annual temperature, whereas there are no significant increasing changes for
366 the temporal analysis. There are also more decreasing changes that are not significant, and fewer
367 increasing non-significant changes, for the temporal analysis relative to the annual temperature results.
368 In comparison with the temporal and annual temperature analyses, the climate indices have fewer
369 significant changes and also more of a mix of increasing and decreasing significant changes. A larger
370 percentage of the non-significant changes are decreasing changes for the temporal analysis and, to a
371 lesser extent, the annual temperature analysis, than for the analyses based on climate indices. These
372 results suggest that the observed temporal and annual temperature-based decreases in nival fraction
373 are not a chance occurrence but rather a response to climate change leading to changes in flood
374 generating processes.

375 [Table 2 near here]

376 Example logistic regression plots are presented in Figure 8 for the analysis based on annual
377 temperature; the sites presented are the four sites used in Figures 2 and 5. Plots for all sites are in Figure
378 S2 in the Supplemental Material. All four sites reveal a decreasing tendency with increasing annual
379 temperature, although only site 40 demonstrates a significant change. In contrast to the even
380 distribution of the predictor variable for the temporal analysis, the annual temperature values are
381 unevenly spaced with a much higher density of values in the central part of the x-axis and isolated
382 values at the low and high extremes. This is particularly noteworthy for site 4 where there is a grouping
383 of three years with mean annual temperatures around 8.3 °C. From these three years, there is one nival
384 event and four pluvial events. Interestingly, the largest of the over threshold events for the year with
385 the largest annual temperature is a nival event (see the upper rug plot of Figure 8c).

386 [Figure 8 near here]

387 Figure 9 presents example logistic regression plots, based on AMO, for the same four sites presented in
388 Figures 2, 5, and 8. The results from AMO as the climate index included in the logistic regression were
389 selected for display since Burn & Whitfield (2017) found the phase of AMO to have an effect on flood
390 events in an analysis based on a subset of the stations used in this work. Figure 9 reveals that while all
391 sites presented show a decreasing tendency, only the results for site 2 are significant and only at the
392 10% significance level. For site 2, there is some grouping, based on AMO, in the series of largest pluvial
393 POT event in each year as can be seen from the rug plot on the lower part of Figure 9b. The results in
394 Figure 9 support the conclusion from Table 2 that the changes in nival fraction related to climate indices
395 are weaker than the temporal changes or the changes based on annual temperature.

396 [Figure 9 near here]

397

398 **4.0 Discussion**

399 The results of this study reveal a preponderance of sites in the study area with a mixture of flood
400 generating processes (i.e., 40 of the 46 sites have both nival and pluvial flood events) and also a mix of
401 nival and pluvial events that are the largest event in a year. A mixture of flood generating processes has
402 implications for flood frequency analysis since traditional approaches to the estimation of extreme flow
403 quantiles assume that the data record consists of independent and identically distributed events, which
404 is generally not true for sites with mixed flood generating processes. Furthermore, an increase in pluvial
405 events was observed for many of the sites implying that not only are there mixed flood generating
406 processes for these sites but also the relative portion of events arising from each process is changing.
407 When conducting flood frequency analysis, it is thus important to consider both the existence of
408 different flood generating processes as well as changes with time in the mixture and frequency of

409 occurrence of flood generating processes. Dividing the flood events into subsets based on flood
410 generating process, however, results in smaller data sets from which to estimate the flood distribution
411 parameters, which increases the uncertainty in the parameter estimates, especially for cases where
412 there is a small number of flood events from one flood generating process. There is clearly a need for
413 further research into methods that can address the complications in flood frequency analysis arising
414 from both mixed flood generating processes and changes in the mix of flood generating processes.

415 The results presented demonstrate clear decreases in the nival fraction over time and with increases in
416 annual temperature, but the temperature trends do not completely explain the temporal pattern of
417 changes in nival fraction. This suggests that the temporal pattern reflects changes in precipitation, and
418 perhaps precipitation form, that is not completely captured in the annual temperature analysis.

419 As noted earlier, the spatial coverage of sites in the study area is sparse. However, the sparse network
420 of sites ensures greater independence in the change responses identified. An examination of the year of
421 occurrence of large flood events at each site reveals that mesoscale events, such as the driver for the
422 2013 Calgary, Alberta flood, are not behind the observed changes.

423 There have been other papers that have examined similar issues to those examined herein. Several of
424 these studies considered a study area that overlaps with the US portion of the study area for this
425 research; there have been fewer studies that have examined similar issues for the Canadian portion of
426 this study. In a study of watersheds in the western United States, Yu *et al*. (2022) examined three flood
427 generating processes, rain, rain-on-snow, and snowmelt, and found that combining flood estimates
428 based on different flood generating mechanisms generally resulted in larger estimates of long return
429 period events in comparison with estimates from considering the flood data to come from a single
430 population. This emphasizes the importance of considering the flood generating process of each flood
431 event when estimating extreme flow quantiles. Hwang & Devineni (2022) used a water balance model

to calculate an index of snow contribution to runoff that shows a similar pattern in their Figure 1 to the nival fraction for the US part of this study as shown in Figure 1 of this paper. The snow contribution index displayed in Hwang & Devineni (2022) contains only three categories and hence is more granular than the nival fraction from this paper; this paper views the flood regime as a continuum. Huang *et al*. (2022) examined watersheds in the western US that are part of the HCDN and found decreased frequency and magnitude of rain-on-snow driven events, increased frequency and magnitude of convective storm driven events and a shift to earlier occurrence of snowmelt driven events. Huang *et al*. (2022) used a pooled approach to estimate trends that combines information from all sites in determining the significance of a trend result. The results from this paper are based on a classification of events as being nival or pluvial, as opposed to the six flood generating processes considered by Huang *et al*. (2022) and is also based on separate change analysis at each site, as oppose to a pooled or combined approach. There are, nonetheless, similarities in the overall results in that this paper also found a decrease in the frequency of nival events and an increased frequency of pluvial events. Dhakal & Palmer (2020) examined changes in the seasonality of annual maximum flood events based on changes in the curricular density for the first and second half of the 60-year data record. They found the emergence of flood events outside of the normal snowmelt season for a collection of sites in the northeast and Midwest United States. Their study area overlaps with the US portion of the study area for this paper with the results being consistent with the findings herein for an increase in the contribution of pluvial events to the flood regime.

Zaerpour *et al*. (2021) explored changes in streamflow regimes for 105 RHBN sites in Canada. Their approach involved applying fuzzy clustering to classify sites into six overlapping groups, such that a site can have partial membership in more than one group. They then looked at changes in the degree of membership of a site in a group using a moving decadal time window and used this as a measure of the change in the streamflow regime for a site. The work of Zaerpour *et al*. (2021) is concerned with

streamflow regimes as opposed to the focus of this paper on flood regimes and their study area encompasses a larger portion of Canada, which then requires the examination of a shorter time period; Zaerpour *et al*. (2021) used a 60-year period versus an 80-year period in this work. Although direct comparison of results from the two studies is challenging due to the differences in the sites considered, methodology, and time period, there are some commonalities. Zaerpour *et al*. (2021) also found shifts to a more pluvial-dominated response for areas where this study has found a strong signal of increases in rainfall contributions to flooding. Whitfield & Shook (2020) investigated changes in precipitation phase associated with autumn precipitation events in the Rocky Mountains of North America. They found mainly increasing trends in rainfall events, which they attributed to winter precipitation shifting to rain. The precipitation shift is consistent with the results for this work although the focus of this work was not exclusively on autumn events. Whitfield & Pomeroy (2016) discuss the flood record for the Bow River at Banff (site 20 in this work) and considered flood events arising from snowmelt and from rain-on-snow. While there were only a small number of rain-on-snow events, they tended to be larger magnitude events. While there is a decreasing trend in the flood event magnitudes for the series of all flood events, there is not a trend in either the snowmelt flood events or the rain-on-snow flood events when considered separately. The work of Whitfield & Pomeroy (2016) highlights the importance of considering flood generation mechanism both for flood frequency analysis and for trend analysis.

Many of the papers cited in this section used data from a Reference Hydrologic Network (RHN). Long, good quality streamflow records from basins in an RHN that are minimally affected by regulation and landuse change, are a fundamental need in the study of climate driven phenomenon (Leopold 1962; Bard *et al*., 2012; Burn *et al*., 2012; Whitfield *et al*., 2012; Zhang *et al*. 2014; Harrigan *et al*., 2018; Dudley *et al*., 2020). Natural streamflow sites that have not met the criteria for inclusion in an RHN often present different trends in floods than do reference sites (Burn & Whitfield, 2016).

There have been many studies looking at the impacts of different climate modes on flooding. Climate modes reflect interannual variations in atmospheric and oceanic conditions that affect weather at a regional scale. Changes in these teleconnections then result in alterations to many aspects of flood events. Many of the studies on the effect of climate modes on flooding have looked at a specific watershed, or a fairly small geographic region (Webb & Bettancourt, 1992), while others encompass a country (Tan & Gan, 2015) or continental scale (Hodgkins *et al*., 2017). The impacts of climate modes on flooding vary with location, with the climate mode considered, and with the phase of the climate mode; there are also cases of interactions between two climate modes (Gobena & Gan, 2009). While some of these studies have found the influence of climate modes on floods to be greater than the temporal trend in flood attributes (Hodgkins *et al*., 2017), in this study we found climate modes to be of lesser importance than the temporal trend in modelling flood regime changes.

5.0 Conclusions

The results from this research indicate an increased influence of rainfall in flood regimes for gauging stations with long term records on relatively pristine watersheds located in the northern portion of the mid-latitudes of North America. The increased rainfall influence is demonstrated through comparisons of the fraction of flood events that are nival for different time periods and confirmed through the use of logistic regression to identify significant changes. The increased rainfall influence is not completely attributable to increased temperature, but rather precipitation changes are likely occurring as well. The significant changes in nival fraction based on time were all decreasing, implying increased influence of rainfall in flood generation. An examination of four climate indices provided no evidence supporting climate modes as a mechanism causing the changes in flood regime.

Mixed flood generating processes and changes in the mix of flood generating processes with time have implications for flood frequency analysis since the assumption of independent and identically distributed data is unlikely to be valid under these conditions. There is a need for further research into appropriate techniques for flood frequency analysis in the presence of multiple and changing flood generation processes, conditions that are likely to occur in many other parts of the world.

Acknowledgements

This research was partially supported by funding provided by the Natural Sciences and Engineering Research Council of Canada (NSERC) through NSERC FloodNet, a strategic research network, and Global Water Futures. We appreciate being able to use the R packages identified in the methods and the contributions of many people to the CSHShydRology package and to the R Development Core Team. The authors appreciate the many helpful comments from two anonymous reviews, which have improved this paper.

References

Agostinelli, C. and U. Lund (2017). R package 'circular': Circular Statistics (version 0.4-93).

Agresti, A. (2013). An introduction to categorical data analysis. 3rd edition, John Wiley & Sons. 742pp.

Archfield, S. A., R. M. Hirsch, A. Viglione and G. Blöschl (2016). "Fragmented patterns of flood change across the United States." Geophysical Research Letters **43**: 10,232- 210,239 DOI: 10.1002/2016GL070590.

522 Arheimer, B. and G. Lindström (2015). "Climate impact on floods: changes in high flows in
523 Sweden in the past and the future (1911–2100)." Hydrology and Earth System Sciences **19**: 771-
524 784 DOI: 10.5194/hess-19-771-2015.

525 Bard, A., B. Renard and M. Lang (2012). Floods in the Alpine areas of Europe. In: Changes in
526 Flood Risk in Europe. Z. W. Kundzewicz [ed]. Wallingford**:** 362-371.

527 Bertola, M., A. Viglione and G. Blöschl (2019). "Informed attribution of flood changes to decadal
528 variation of atmospheric, catchment and river drivers in Upper Austria." Journal of Hydrology
529 **577**: 123919 DOI: 10.1016/j.jhydrol.2019.123919.

530 Blöschl, G., J. Hall, J. Parajka, R. A. P. Perdigão, B. Merz, B. Arheimer, G. T. Aronica, A. Bilibashi,
531 O. Bonacci, M. Borga and *et al.* (2017). "Changing climate shifts timing of European floods."
532 Science **357**(6351): 588-590 DOI: 10.1126/science.aan2506.

533 Brimley, B., J.-F. Cantin, D. Harvey, M. Kowalchuk, P. Marsh, T. M. B. J. Ouarda, B. Phinney, P.
534 Pilon, M. Renouf, B. Tassone, R. Wedel and T. Yuzyk (1999). Establishment of the reference
535 hydrometric basin network (RHBN) for Canada. Ottawa, Environment Canada**:** 41 pp.

536 Burn, D. H. and N. W. Arnell (1993). "Synchronicity in global flood responses." Journal of
537 Hydrology **144**: 381-404 DOI: 10.1016/0022-1694(93)90181-8.

538 Burn, D. H., J. Hannaford, G. A. Hodgkins, P. H. Whitfield, R. Thorne and T. J. Marsh (2012).
539 "Hydrologic Reference Networks II. Using Reference Hydrologic Networks to assess climate
540 driven changes in streamflow." Hydrological Sciences Journal **57**: 1580-1593 DOI:
541 10.1080/02626667.2012.728705.

Burn, D. H. and P. H. Whitfield (2016). "Changes in floods and flood regimes in Canada." Canadian Water Resources Journal **41**: 139-150 DOI: 10.1080/07011784.2015.1026844.

Burn, D. H. and P. H. Whitfield (2017). "Changes in cold region flood regimes inferred from long record reference gauging stations." Water Resources Research **53**(4): 2643-2658 DOI: 10.1002/2016WR020108.

Burn, D. H. and P. H. Whitfield (2018). "Changes in flood events inferred from centennial length streamflow data records." Advances in Water Resources **121**: 333-349 DOI: 10.1016/j.advwatres.2018.08.017.

Burn, D. H., P. H. Whitfield and M. Sharif (2016). "Identification of changes in floods and flood regimes in Canada using a peaks over threshold approach." Hydrological Processes **39**: 3303-3314 DOI: 10.1002/hyp.10861.

Cunderlik, J. M. and T. M. B. J. Ouarda (2009). "Trends in the timing and magnitude of floods in Canada." Journal of Hydrology **375**: 471-480 DOI: 10.1016/j.jhydrol.2009.06.050.

Dhakal, N. and R. N. Palmer (2020). "Changing River Flood Timing in the Northeastern and Upper Midwest United States: Weakening of Seasonality over Time?" Water **12**(7): 1951 DOI: 10.3390/w12071951.

Dudley, R. W., R. M. Hirsch, S. A. Archfield, A. G. Blum and B. Renard (2020). "Low streamflow trends at human-impacted and reference basins in the United States." Journal of Hydrology **580**: 124254 DOI: 10.1016/j.jhydrol.2019.124254.

Franks, S. W. (2002). "Identification of a change in climate state using regional flood data." Hydrology and Earth System Sciences **6**(1): 11-16 DOI: 10.5194/hess-6-11-2002.

563 Frei, C. and C. Schär (2001). "Detection probability of trends in rare events: Theory and
564 application to heavy precipitation in the Alpine region." Journal of Climate **14**: 1568-1584 DOI:
565 10.1175/1520-0442(2001)014<1568:DPOTIR>2.0.CO;2.

566 Ganguli, P., Y. R. Nandamuri and C. Chatterjee (2020). "Analysis of persistence in the flood
567 timing and the role of catchment wetness on flood generation in a large river basin in India."
568 Theoretical and Applied Climatology **139**: 373–388 DOI: 10.1007/s00704-019-02964-z.

569 Gobena, A. K. and T. Y. Gan (2009). "The Role of Pacific Climate on Low-Frequency
570 Hydroclimatic Variability and Predictability in Southern Alberta, Canada." Journal of
571 Hydrometeorology **10**: 1465-1478 DOI: 10.1175/2009JHM1119.1.

572 Hamlet, A. F. and D. P. Lettenmaier (1999). "Effects of climate change on hydrology and water
573 resources of the Columbia River basin." Journal of the American Water Resources Association
574 **35**: 1507-1623 DOI: 10.1111/j.1752-1688.1999.tb04240.x.

575 Hanus, S., M. Hrachowitz, H. Zekollari, G. Schoups, M. Vizcaino and R. Kaitna (2021). "Timing
576 and magnitude of future annual runoff extremes in contrasting Alpine catchments in Austria."
577 Hydrology and Earth System Sciences Discussions: 1-35 DOI: 10.5194/hess-2021-92.

578 Harrigan, S., J. Hannaford, K. Muchan and T. J. Marsh (2018). "Designation and trend analysis of
579 the updated UK Benchmark Network of river flow stations: the UKBN2 dataset." Hydrology
580 Research **49**(2): 552-567 DOI: 10.2166/nh.2017.058.

581 Hodgkins, G. A., P. H. Whitfield, D. H. Burn, J. Hannaford, B. Renard, K. Stahl, A. K. Fleig, H.
582 Madsen, L. Mediero, J. Korhonen, C. Murphy and D. Wilson (2017). "Climate-driven trends in

583 the occurrence of major floods across North America and Europe." Journal of Hydrology **552**:
584 704-717 DOI: 10.1016/j.jhydrol.2017.07.027.

585 Huang, H., M. R. Fischella, Y. Liu, Z. Ban, J. V. Fayne, D. Li, K. C. Cavanaugh and D. P. Lettenmaier
586 (2022). "Changes in mechanisms and characteristics of western US floods over the last sixty
587 years." Geophysical Research Letters **49**(3): e2021GL097022 DOI: 10.1029/2021GL097022.

588 Huntington, T. G. (2006). "Evidence for intensification of the global water cycle: review and
589 synthesis." Journal of Hydrology **319**(1-4): 83-95 DOI: 10.1016/j.jhydrol.2005.07.003.

590 Hwang, J. and N. Devineni (2022). "An improved Zhang's Dynamic Water Balance Model using
591 Budyko-based snow representation for better streamflow predictions." Water Resources
592 Research **58**(1): e2021WR030203 DOI: 10.1029/2021WR030203.

593 Jain, S. and U. Lall (2000). "Magnitude and timing of annual maximum floods: trends and large-
594 scale climatic associations for the Blacksmith Fork River, Utah." Water Resources Research
595 **36**(12): 3641-3651 DOI: 10.1029/2000WR900183.

596 Köplin, N., B. Schädler, D. Viviroli and R. Weingartner (2014). "Seasonality and magnitude of
597 floods in Switzerland under future climate change." Hydrological Processes **28**: 2567-2578 DOI:
598 10.1002/hyp.9757.

599 Kundzewicz, Z. W., M. Szwed and I. Pińskwar (2019). "Climate Variability and Floods—A Global
600 Review." Water **11**(7): 1399 DOI: 10.3390/w11071399.

601 Lang, M., T. M. B. J. Ouarda and B. Bobée (1999). "Towards operational guidelines for over-
602 threshold modeling." Journal of Hydrology **225**: 103-117 DOI: 10.1016/S0022-1694(99)00167-5.

Lang, M., B. Renard, E. Sauquet, P. Bois, A. Dupeyrat, C. Laurent, O. Mestre, H. Niel, L. Neppel and J. Gailhard (2006). "A national study on trends and variations of French floods and droughts." IAHS PUBLICATION **308**: 514.

Leopold, L. B. (1962). "A national network of hydrologic bench marks." USGS Conservation Networks Geological Circular 460-B: 4pp.

Lins, H. F. (2012). "USGS hydro-climatic data network 2009 (HCDN-2009)." US Geological Survey Fact Sheet **3047**(4) DOI: 10.3133/fs20123047.

Liu, J., Q. Zhang, V. P. Singh, X. Gu and P. Shi (2017). "Nonstationarity and clustering of flood characteristics and relations with the climate indices in the Poyang Lake basin, China." Hydrological Sciences Journal **62**(11): 1809-1824 DOI: 10.1080/02626667.2017.1349909.

Maechler, M., P. J. Rousseeuw, A. Struyf, M. Hubert and K. M. Hornik (2019). "cluster: Cluster Analysis Basics and Extensions." R package version **2**(0).

Mallakpour, I. and G. Villarini (2015). "The changing nature of flooding across the central United States." Nature Climate Change **5**: 250–254 DOI: 10.1038/nclimate2516.

Mediero, L., D. Santillán, L. Garrote and A. Granados (2014). "Detection and attribution of trends in magnitude, frequency and timing of floods in Spain." Journal of Hydrology **517**: 1072-1088 DOI: 10.1016/j.jhydrol.2014.06.040.

Merz, B., N. V. Dung, H. Apel, L. Gerlitz, K. Schröter, E. Steirou and S. Vorogushyn (2018). "Spatial coherence of flood-rich and flood-poor periods across Germany." Journal of Hydrology **559**: 813-826 DOI: 10.1016/j.jhydrol.2018.02.082.

623 Pan, X., A. Rahman, K. Haddad and T. B. M. J. Ouarda (2022). "Peaks-over-threshold model in
624 flood frequency analysis: a scoping review." Stochastic Environmental Research and Risk
625 Assessment: 1-17 DOI: 10.1007/s00477-022-02174-6.

626 Pewsey, A., M. Neuhäuser and G. D. Ruxton (2014). Circular Statistics in R, Oxford University
627 Press.

628 R_Core_Team (2021). R: A language and environment for statistical computing. Vienna, Austria,
629 R Foundation for Statistical Computing.

630 Renard, B., M. Lang, P. Bois, A. Dupeyrat, O. Mestre, H. Niel, E. Sauquet, C. Prudhomme, S.
631 Parey, E. Paquet, L. Neppel and J. Gailhard (2008). "Regional methods for trend detection:
632 Assessing field significance and regional consistency." Water Resources Research **44** DOI:
633 10.1029/2007/WR006268.

634 Reynolds, A. P., G. Richards, B. de la Iglesia and V. J. Rayward-Smith (2006). "Clustering Rules: A
635 Comparison of Partitioning and Hierarchical Clustering Algorithms." Journal of Mathematical
636 Modelling and Algorithms **5**: 475-504 DOI: 10.1007/s10852-005-9022-1.

637 Rokaya, P., S. Budhathoki and K.-E. Lindenschmidt (2018). "Trends in the Timing and Magnitude
638 of Ice-Jam Floods in Canada." Scientific reports **8**(1): 5834 DOI: 10.1038/s41598-018-24057-z.

639 Sankarasubramanian, A. and U. Lall (2003). "Flood quantiles in a changing climate: Seasonal
640 forecasts and causal relations." Water Resources Research **39**(5) DOI: 10.1029/2002WR001593.

641 Sharma, A., C. Wasko and D. P. Lettenmaier (2018). "If precipitation extremes are increasing,
642 why aren't floods?" Water Resources Research **54**(11): 8545-8551 DOI:
643 10.1029/2018WR023749.

644 Tan, X. and T. Y. Gan (2015). "Nonstationary Analysis of Annual Maximum Streamflow of
645 Canada." Journal of Climate **28**(5): 1788–1805 DOI: 10.1175/JCLI-D-14-00538.1.
646 Trenberth, K. E. (2005). "The impact of climate change and variability on heavy precipitation,
647 floods, and droughts." In: M.G. Anderson (ed.), Encyclopedia of Hydrological Sciences: 1-11 DOI:
648 10.1002/0470848944.hsa211.
649 Veijalainen, N., E. Lotsari, P. Alho, B. Vehviläinen and J. Käyhkö (2010). "National scale
650 assessment of climate change impacts on flooding in Finland." Journal of Hydrology **391**(3):
651 333-350 DOI: 10.1016/j.jhydrol.2010.07.035.
652 Vormoor, K., D. Lawrence, M. Heistermann and A. Bronstert (2016). "Climate change impacts on
653 the seasonality and generation processes of floods in catchments with mixed snowmelt/rainfall
654 regimes: projections and uncertainties." Hydrology and Earth System Sciences **19**: 913-931 DOI:
655 10.5194/hess-19-913-2015.
656 Wang, T., A. Hamann, D. L. Spittlehouse and C. Carroll (2016). "Locally Downscaled and Spatially
657 Customizable Climate Data for Historical and Future Periods for North America." PLoS ONE
658 **11**(6) DOI: 10.1371/journal.pone.0156720.
659 Wang, T., A. Hamann, D. L. Spittlehouse and T. Q. Murdock (2012). "ClimateWNA – High-
660 resolution spatial climate data for western North America." Journal of Applied Meteorology and
661 Climatology **51**: 16-29 DOI: 10.1175/JAMC-D-11-043.1.
662 Webb, R. H. and J. L. Betancourt (1992). "Climatic variability and flood frequency of the Santa
663 Cruz River, Pima County, Arizona." U.S. Geological Survey Water Supply Paper 2379 40 pp. DOI:
664 10.3133/wsp2379.

Whitfield, P. H. (2012). "Floods in Future Climates: A Review." Journal of Flood Risk Management **5**: 336-365 DOI: 10.1111/j.1753-318X.2012.01150.x.

Whitfield, P. H. (2018). "Clustering of seasonal events: A simulation study using circular methods." Communications in Statistics - Simulation and Computation **47**(10): 3008-3030 DOI: 10.1080/03610918.2017.1367805.

Whitfield, P. H., D. H. Burn, J. Hannaford, H. Higgins, G. A. Hodgkins, T. Marsh and U. Looser (2012). "Hydrologic Reference Networks I. The Status of National Reference Hydrologic Networks for Detecting Trends and Future Directions." Hydrological Sciences Journal **57**: 1562-1579 DOI: 10.1080/02626667.2012.728706.

Whitfield, P. H. and J. W. Pomeroy (2016). "Changes to flood peaks of a mountain river: implications for analysis of the 2013 flood in the Upper Bow River, Canada." Hydrological Processes **30**: 4657-4673 DOI: 10.1002/hyp.10957.

Whitfield, P. H. and K. R. Shook (2020). "Changes to rainfall, snowfall, and runoff events during the autumn-winter transition in the Rocky Mountains of North America." Canadian Water Resources Journal **45**(1): 28-42 DOI: 10.1080/07011784.2019.1685910.

Yu, G., D. B. Wright and F. V. Davenport (2022). "Diverse Physical Processes Drive Upper-Tail Flood Quantiles in the US Mountain West." Geophysical Research Letters **49**(10): e2022GL098855 DOI: 10.1029/2022GL098855.

Zaerpour, M., S. Hatami, J. Sadri and A. Nazemi (2021). "A global algorithm for identifying changing streamflow regimes: application to Canadian natural streams (1966–2010)." Hydrology and Earth System Sciences **25**(9): 5193-5217 DOI: 10.5194/hess-25-5193-2021.

686 Zhang, S. X., M. Bari, G. Amirthanathan, D. Kent, A. MacDonald and D. Shin (2014). “Hydrologic
687 Reference Stations to Monitor Climate-Driven Streamflow Variability and Trends.” Hydrology
688 and Water Resources Symposium 2014, Engineers Australia.

689 Zhang, Q., X. Gu, V. P. Singh, P. Shi and M. Luo (2017). "Timing of floods in southeastern China:
690 seasonal properties and potential causes." Journal of Hydrology **552**: 732-744 DOI:
691 10.1016/j.jhydrol.2017.07.039.

692 Zhang, Q., X. Gu, V. P. Singh, P. Siun, X. Chen and D. Kong (2016). "Magnitude, frequency and
693 timing of floods in the Tarim River basin, China: Changes, causes and implications." Global and
694 Planetary Change **139**: 44-55 DOI: 10.1016/j.gloplacha.2015.10.005.

Figures

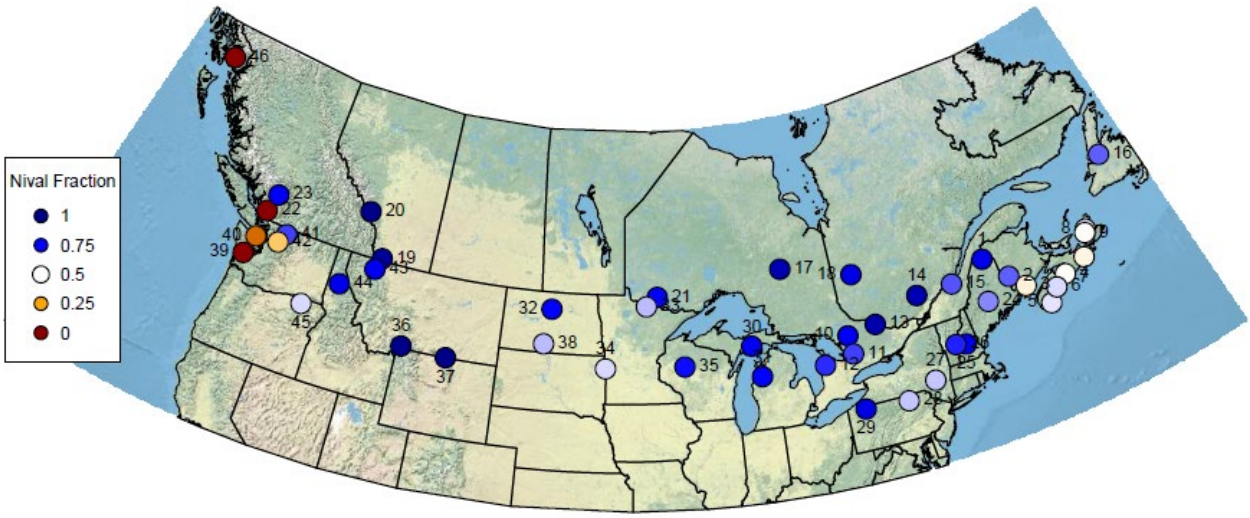

Figure 1 Station locations with site numbers. The colour indicates the nival fraction for the period of record for a site.

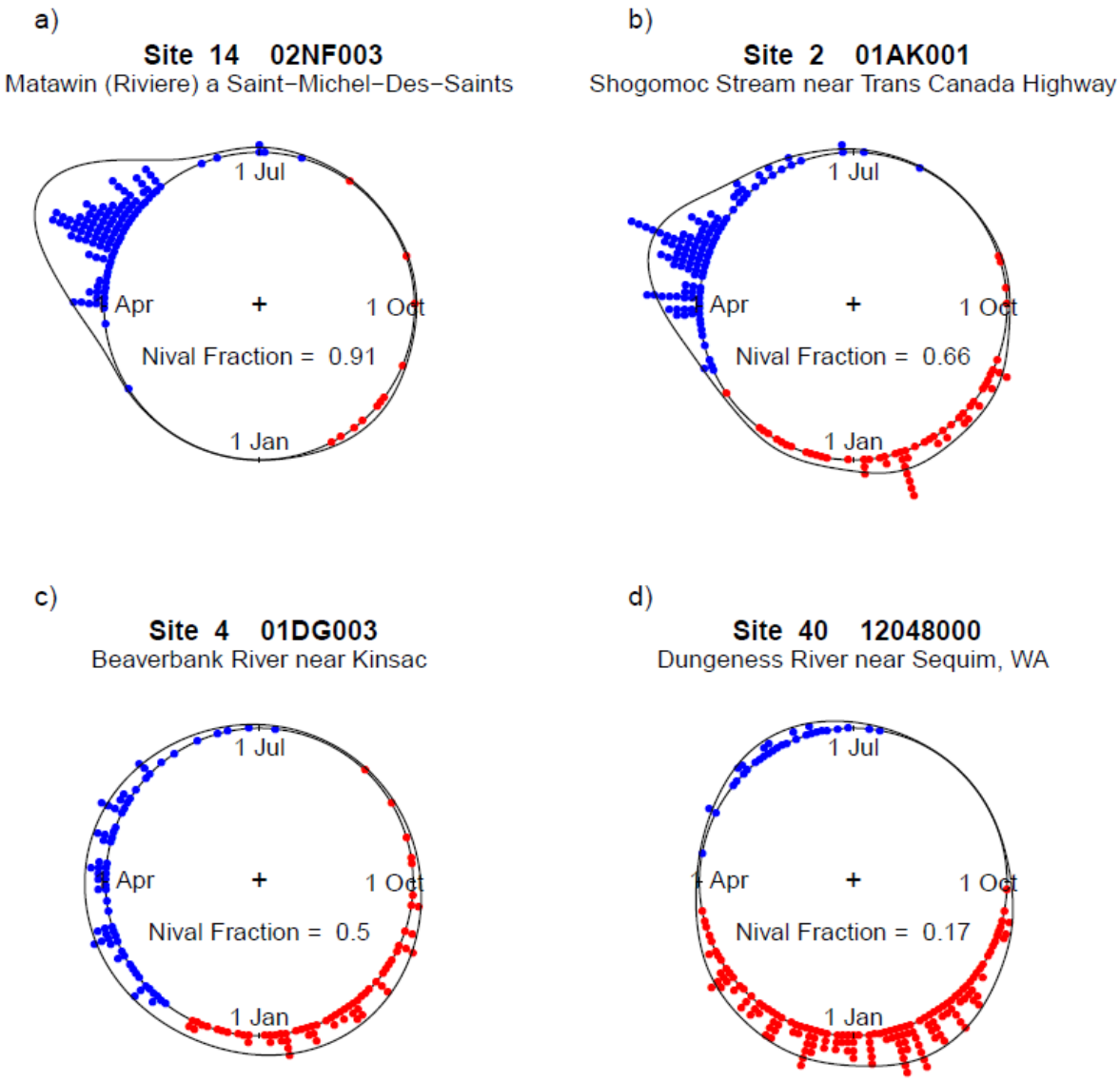

Figure 2 Examples of the clustering of POT events for four sites with differing nival fractions. Points are stacked around the unit circle and placed in bins with a bin size of two days. Nival events are blue dots and pluvial events are red dots. The solid lines denote the kernel density estimate for the circular distribution of the occurrence of over threshold events. Plots a) through d) depict sites with decreasing nival fraction.

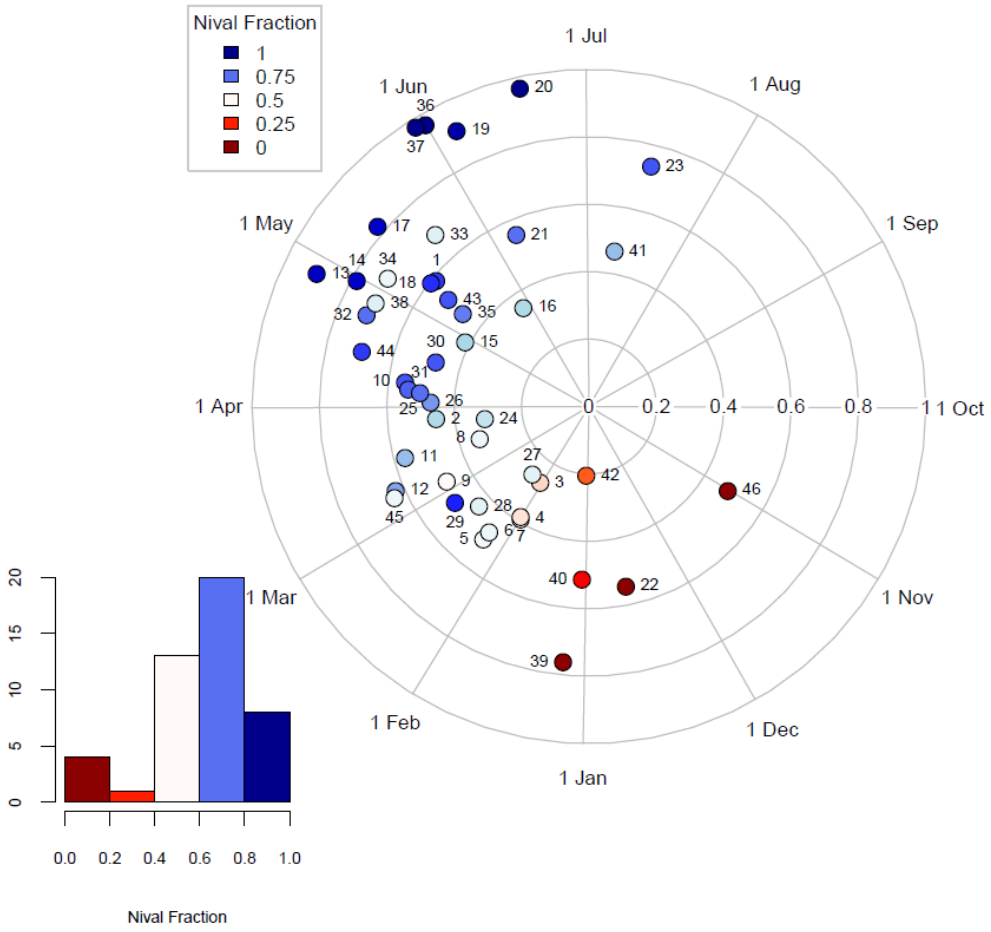

708

709 Figure 3 Polar plot of the 46 stations indicating the mean day of year of the POT events, and the

710 regularity in the radial direction. Symbol colours indicate the nival fraction. The histogram in the lower

711 left shows the counts of stations based on nival fraction.

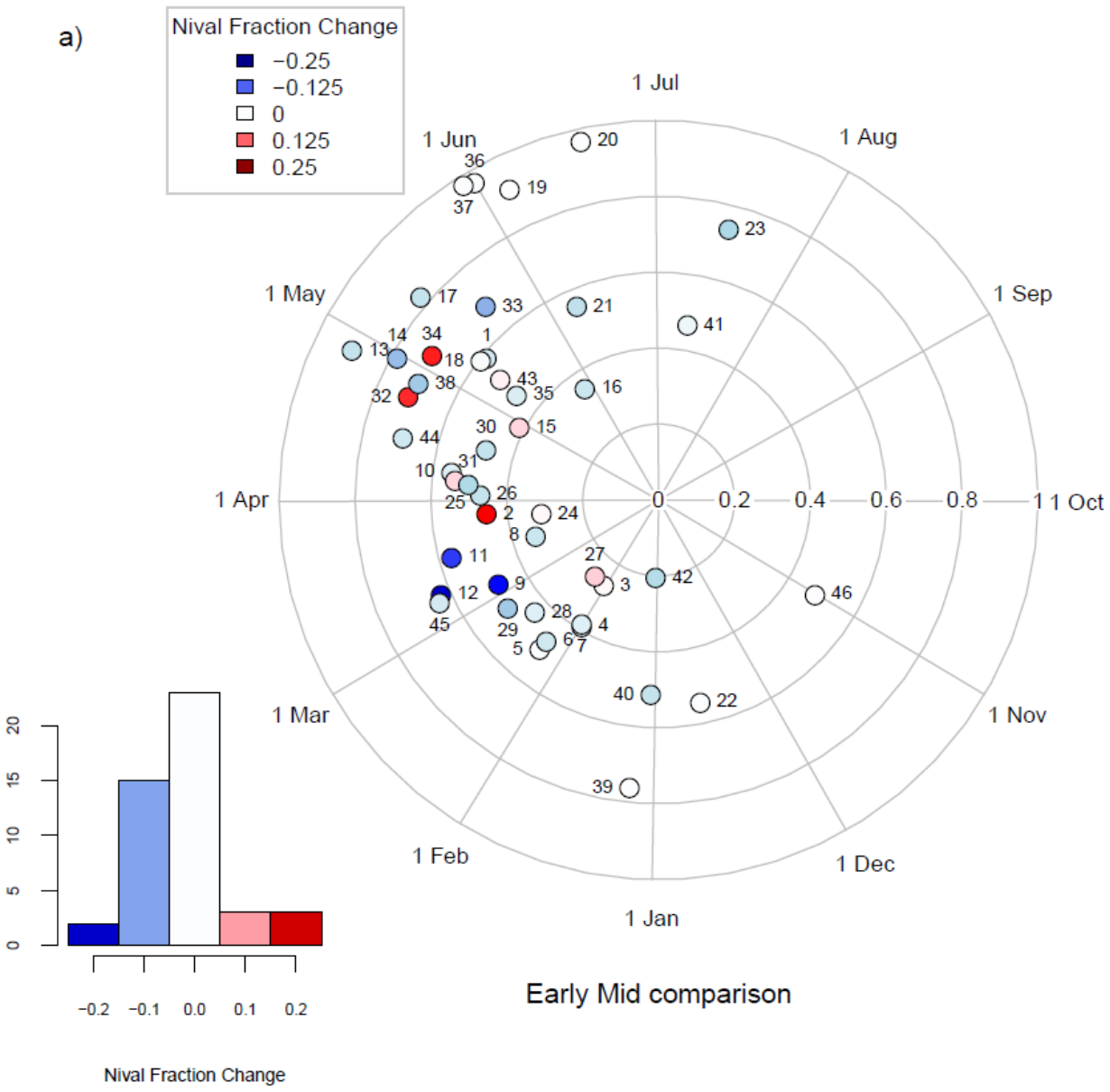
a)
Nival Fraction Change
−0.25
−0.125
0
0.125
0.25
1 Jul
1 Aug
1 Sep
1 Oct
1 Nov
1 Dec
1 Jan
1 Feb
1 Mar
1 Apr
1 May
1 Jun
0
0.2
0.4
0.6
0.8
1
0
5
10
15
20
−0.2
−0.1
0.0
0.1
0.2
Nival Fraction Change
Early Mid comparison

712

b)

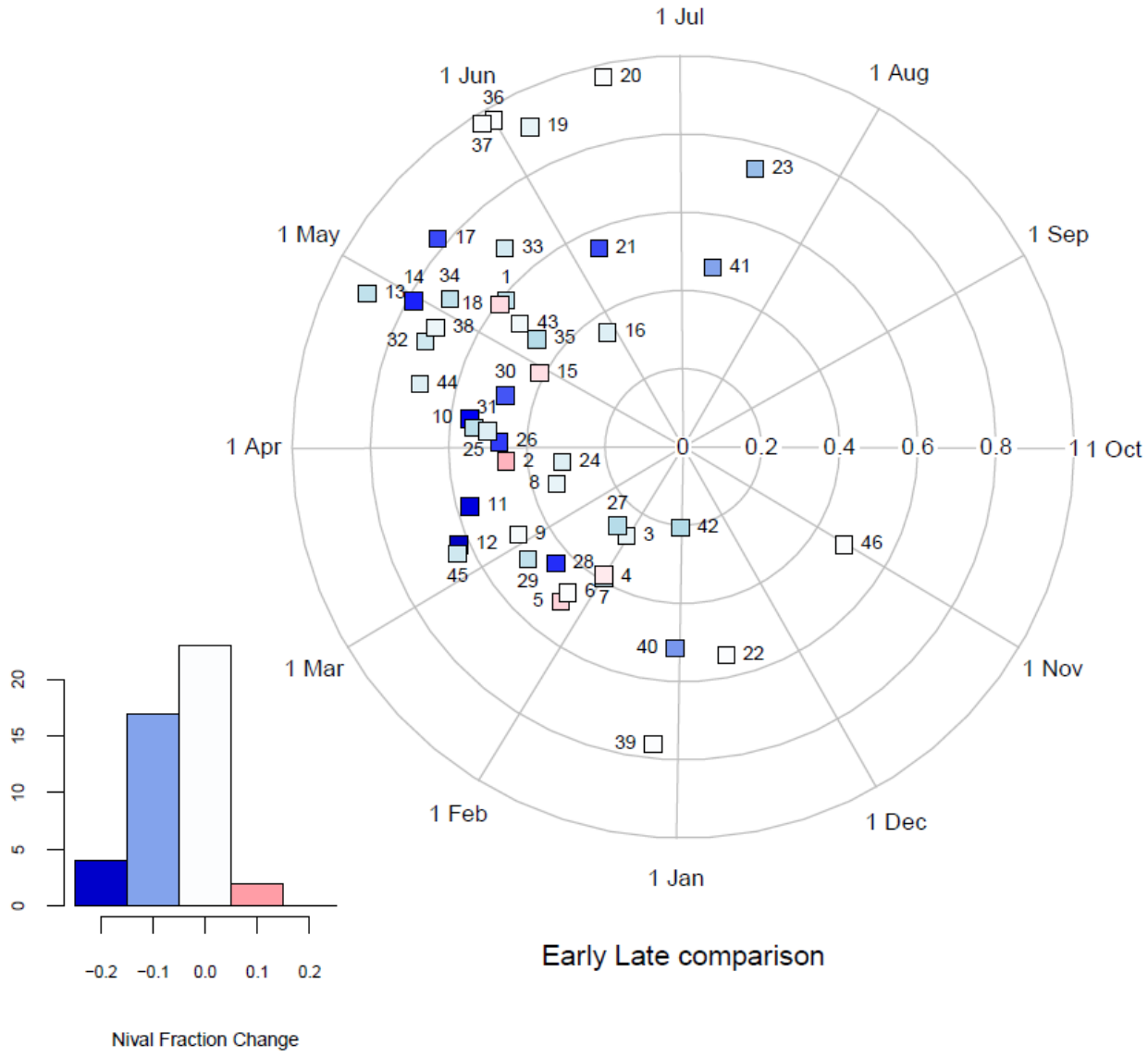
1 Jul
1 Aug
1 Sep
1 Oct
1 Nov
1 Dec
1 Jan
1 Feb
1 Mar
1 Apr
1 May
1 Jun
0
0.2
0.4
0.6
0.8
1
Early Late comparison
Nival Fraction Change
−0.2
−0.1
0.0
0.1
0.2
0
5
10
15
20

713

c)

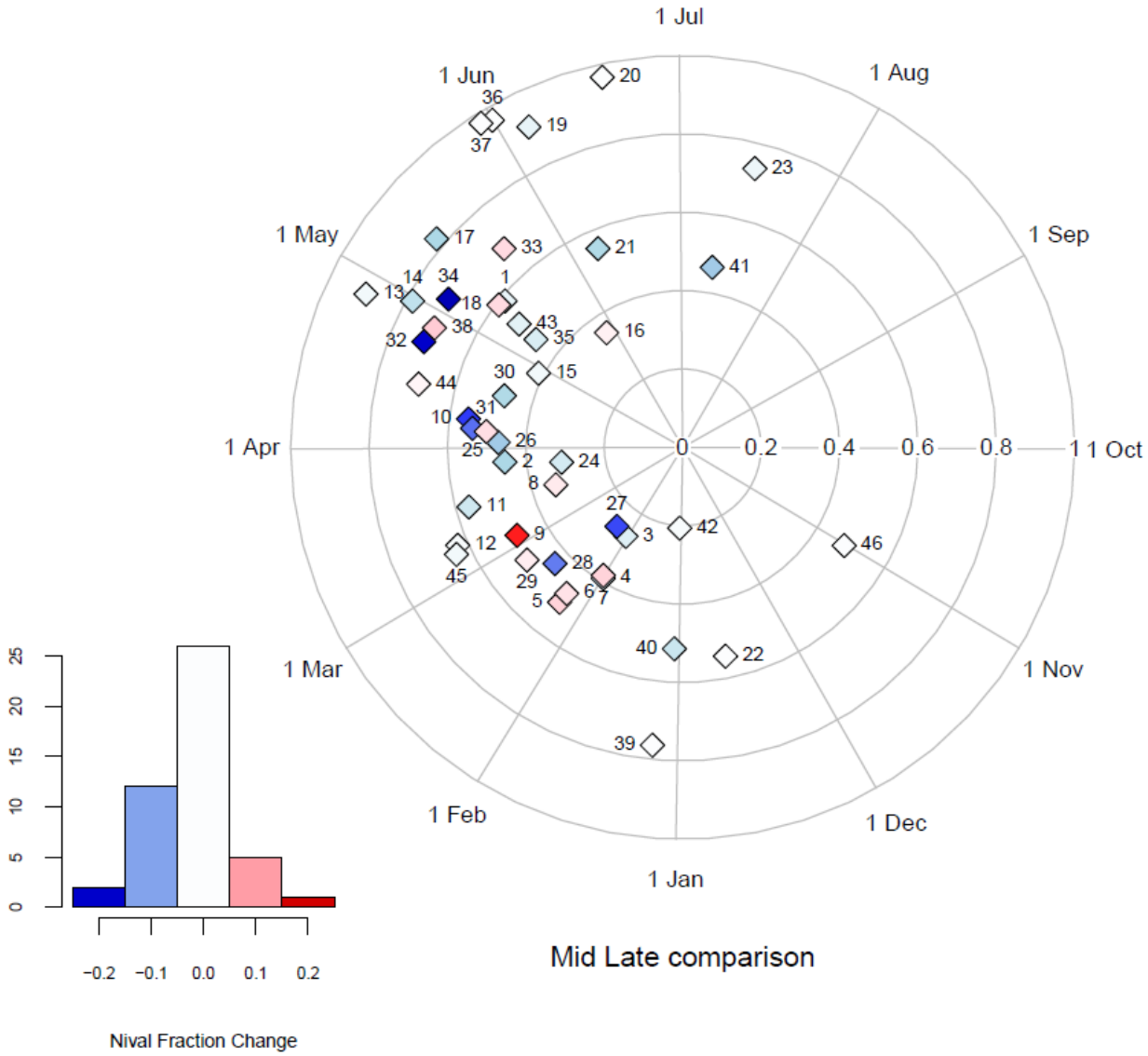
1 Jul
1 Jun
1 Aug
1 May
1 Sep
1 Apr
1 Oct
1 Mar
1 Nov
1 Feb
1 Dec
1 Jan
0
0.2
0.4
0.6
0.8
1
Mid Late comparison
0
5
10
15
20
25
−0.2
−0.1
0.0
0.1
0.2
Nival Fraction Change

714

d)

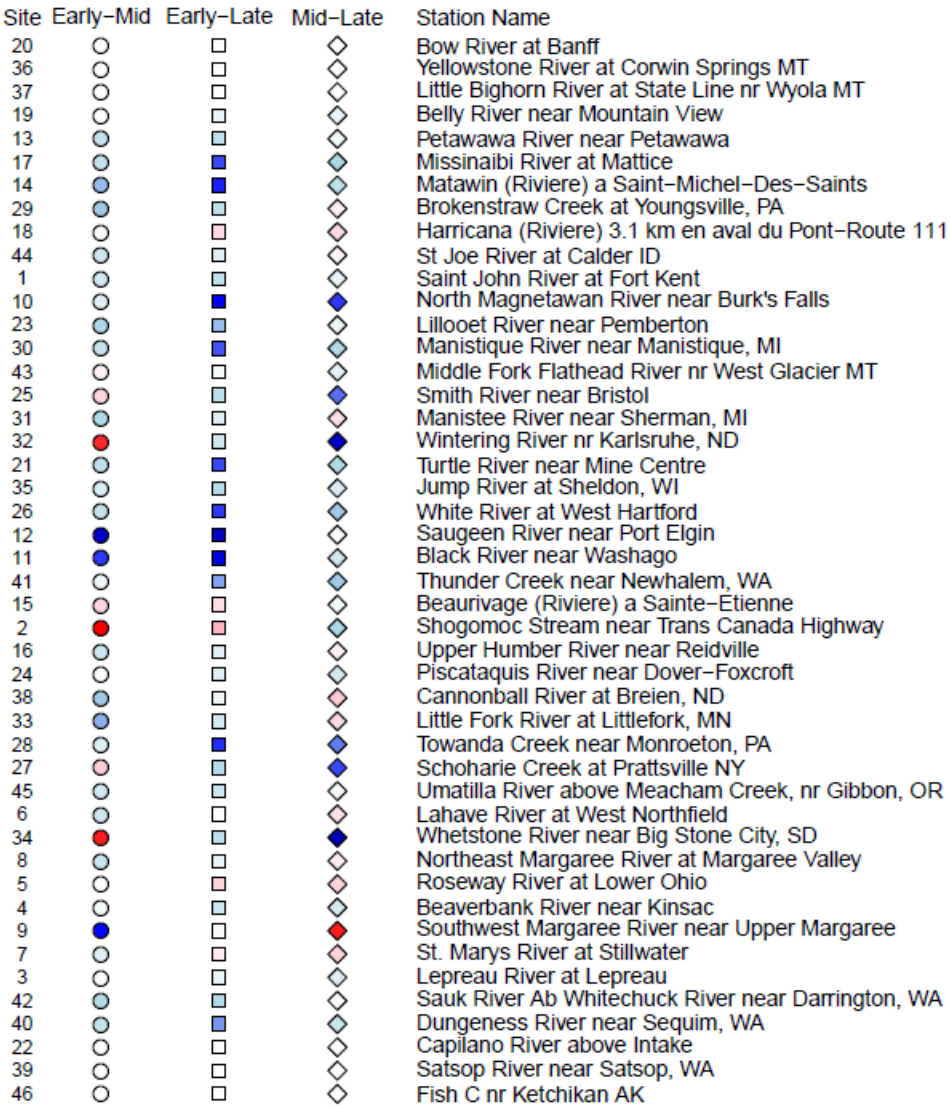

Site	Early–Mid	Early–Late	Mid–Late	Station Name
20				Bow River at Banff
36				Yellowstone River at Corwin Springs MT
37				Little Bighorn River at State Line nr Wyola MT
19				Belly River near Mountain View
13				Petawawa River near Petawawa
17				Missinaibi River at Mattice
14				Matawin (Riviere) a Saint–Michel–Des–Saints
29				Brokenstraw Creek at Youngsville, PA
18				Harricana (Riviere) 3.1 km en aval du Pont–Route 111
44				St Joe River at Calder ID
1				Saint John River at Fort Kent
10				North Magnetawan River near Burk's Falls
23				Lillooet River near Pemberton
30				Manistique River near Manistique, MI
43				Middle Fork Flathead River nr West Glacier MT
25				Smith River near Bristol
31				Manistee River near Sherman, MI
32				Wintering River nr Karlsruhe, ND
21				Turtle River near Mine Centre
35				Jump River at Sheldon, WI
26				White River at West Hartford
12				Saugeen River near Port Elgin
11				Black River near Washago
41				Thunder Creek near Newhalem, WA
15				Beaurivage (Riviere) a Sainte–Etienne
2				Shogomoc Stream near Trans Canada Highway
16				Upper Humber River near Reidville
24				Piscataquis River near Dover–Foxcroft
38				Cannonball River at Breien, ND
33				Little Fork River at Littlefork, MN
28				Towanda Creek near Monroeton, PA
27				Schoharie Creek at Prattsville NY
45				Umatilla River above Meacham Creek, nr Gibbon, OR
6				Lahave River at West Northfield
34				Whetstone River near Big Stone City, SD
8				Northeast Margaree River at Margaree Valley
5				Roseway River at Lower Ohio
4				Beaverbank River near Kinsac
9				Southwest Margaree River near Upper Margaree
7				St. Marys River at Stillwater
3				Lepreau River at Lepreau
42				Sauk River Ab Whitechuck River near Darrington, WA
40				Dungeness River near Sequim, WA
22				Capilano River above Intake
39				Satsop River near Satsop, WA
46				Fish C nr Ketchikan AK

715

716 Figure 4. Polar plot of the 46 stations indicating the mean day of year of the POT events and the
717 regularity in the radial direction. Symbols are colour coded to indicate change in nival fraction between:
718 a) early and mid section of the period; b) early and late section of the period; and c) mid and late section
719 of the period. The changes for each segment are highlighted in panel d) where the sites are ordered by
720 decreasing nival fraction. The symbols in d) correspond to the symbols for the different segment
721 comparisons in parts a), b) and c).

722

723 -

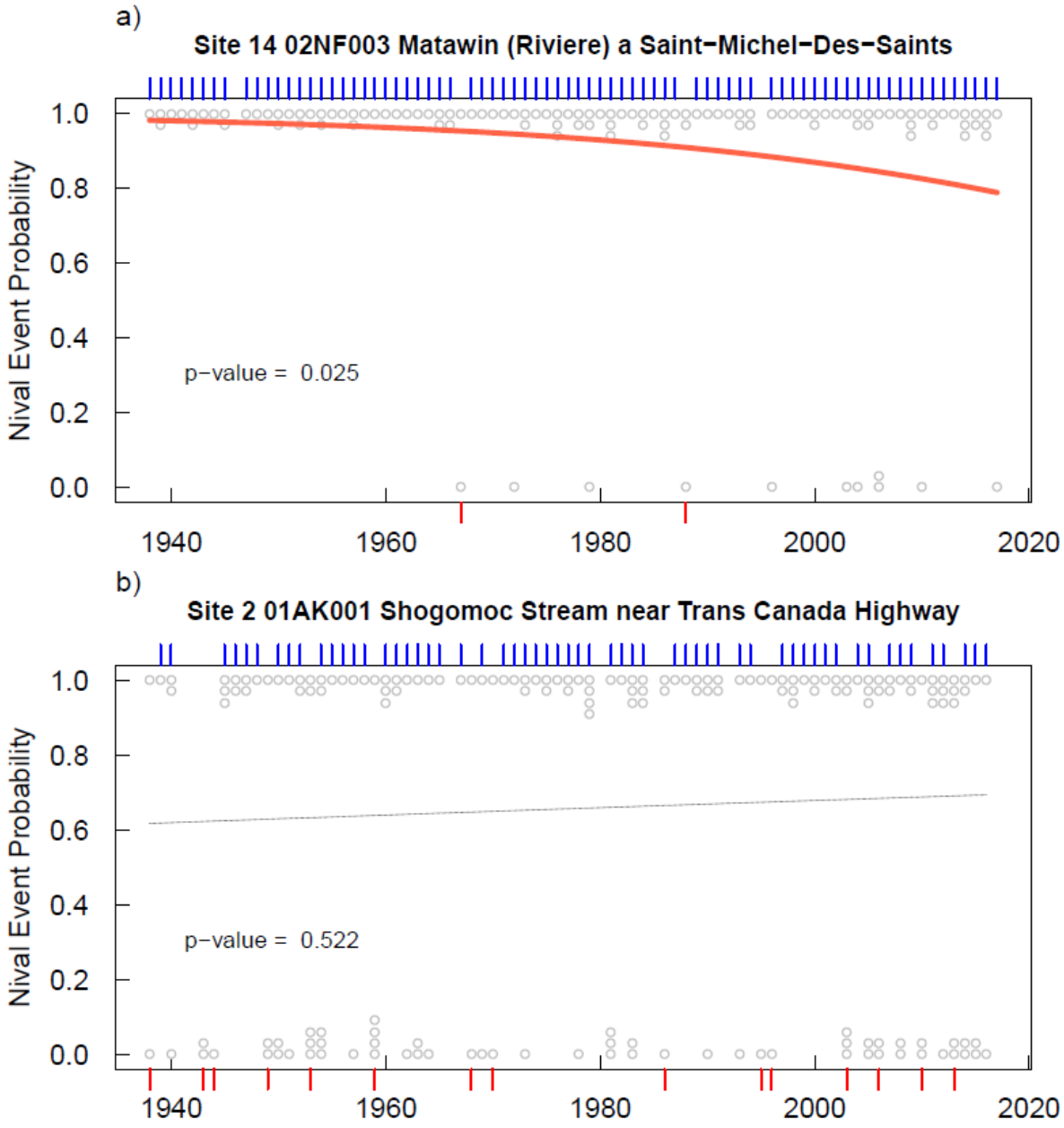
a)
Site 14 02NF003 Matawin (Riviere) a Saint−Michel−Des−Saints
Nival Event Probability
1.0
0.8
0.6
0.4
0.2
0.0
p−value = 0.025
1940
1960
1980
2000
2020
b)
Site 2 01AK001 Shogomoc Stream near Trans Canada Highway
Nival Event Probability
1.0
0.8
0.6
0.4
0.2
0.0
p−value = 0.522
1940
1960
1980
2000
2020

724

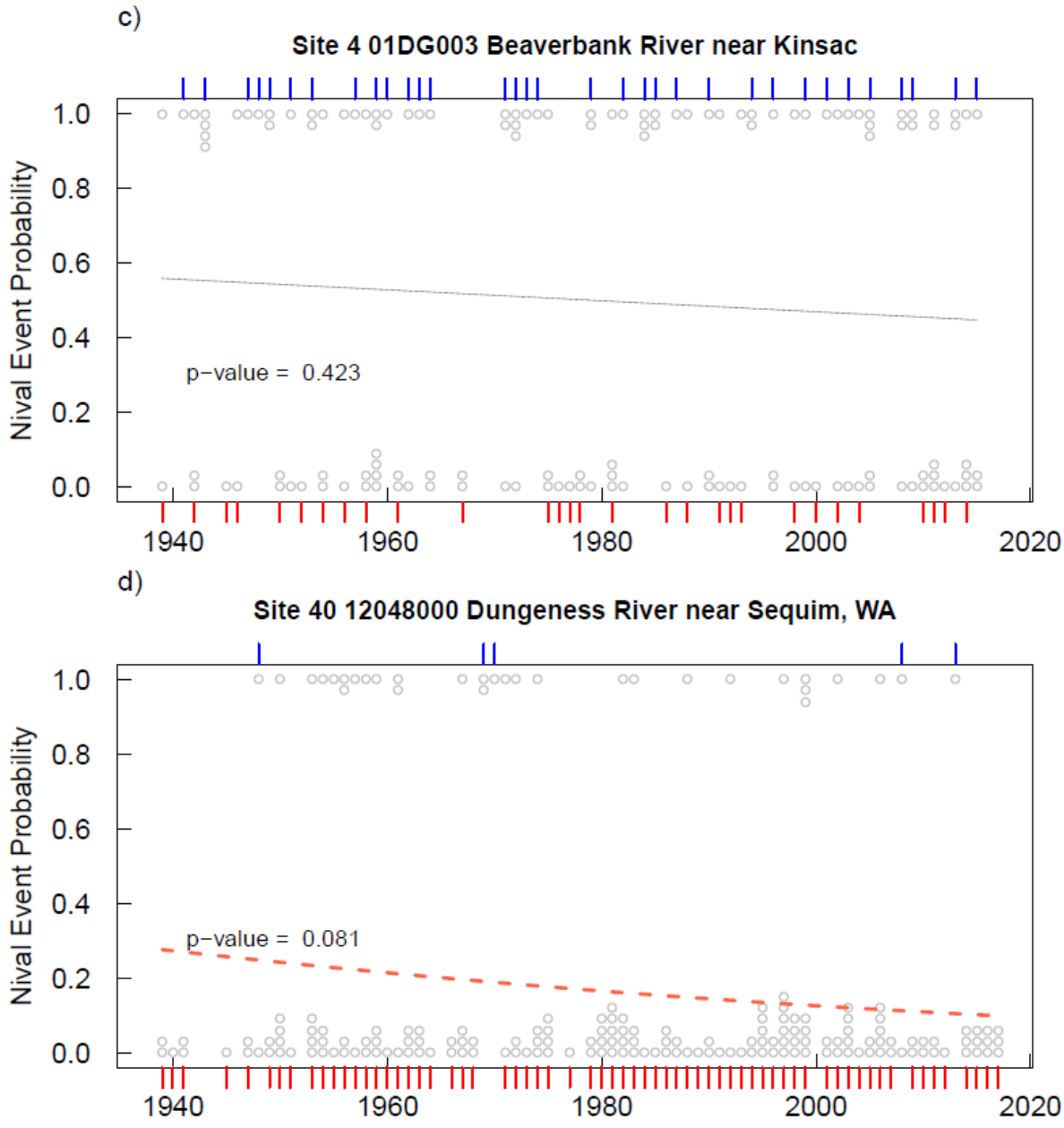

Figure 5 Time series of POT events and the results of the logistic regression. POT events are shown as gray circles either stacked at nival event probability of 1.0 (nival events) or 0.0 (pluvial events). The largest POT event in each year is shown outside the frame as nival (blue, top), or pluvial (red, bottom) tick marks. The line of the logistic regression is solid red if the p value is ≤ 0.05; dashed red if the p value is > 0.05 but ≤ 0.10, and light gray otherwise. Figure S1 in the Supplementary Material provides results for each of the 46 sites.

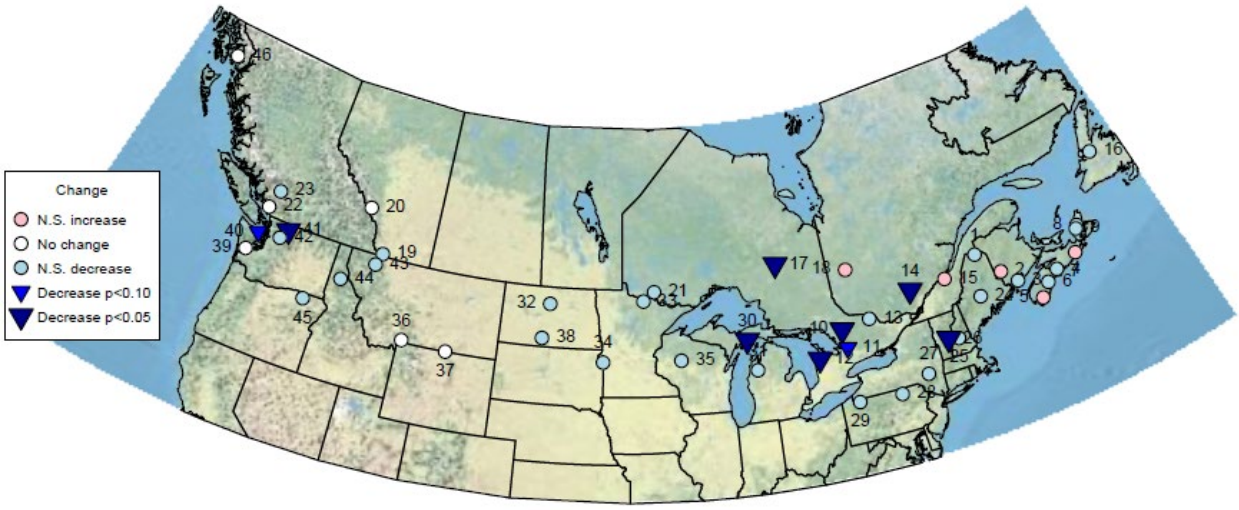

732

733 Figure 6 Map of the results of the logistic regression analysis for changes in nival fraction of POT events

734 over time. Downward triangles indicate decreasing changes in nival events. No increasing changes were

735 significant.

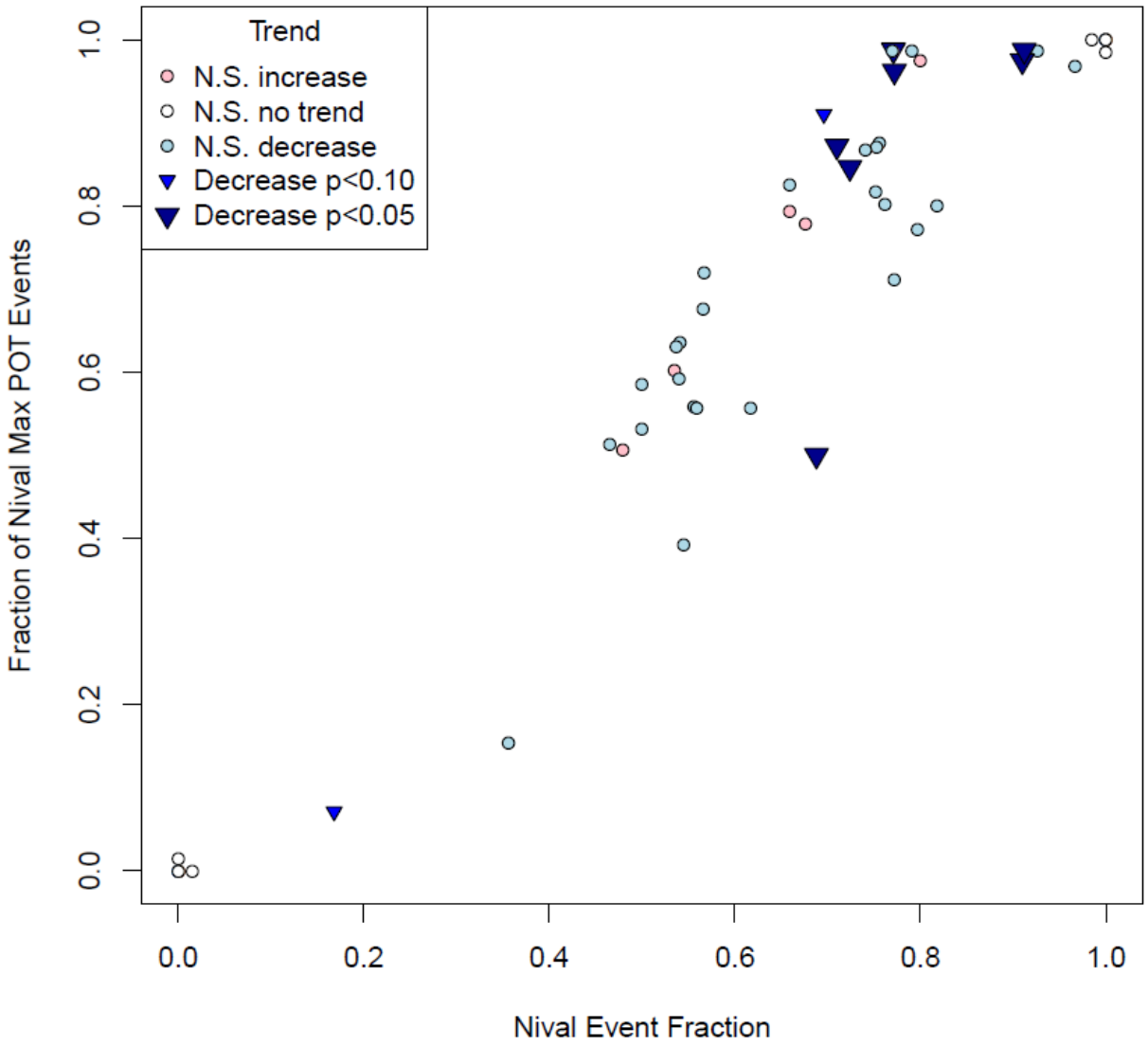

736

737 Figure 7 Plot of the fraction of maximum POT events that are nival versus the fraction of nival POT

738 events. All sites have at least one nival maximum POT event and at least one pluvial maximum POT

739 event with the exception of the three sites that plot at (0,0), corresponding to sites with all pluvial POT

740 events, and the three sites that plot at (1,1), corresponding to sites with all nival POT events.

741

742

743

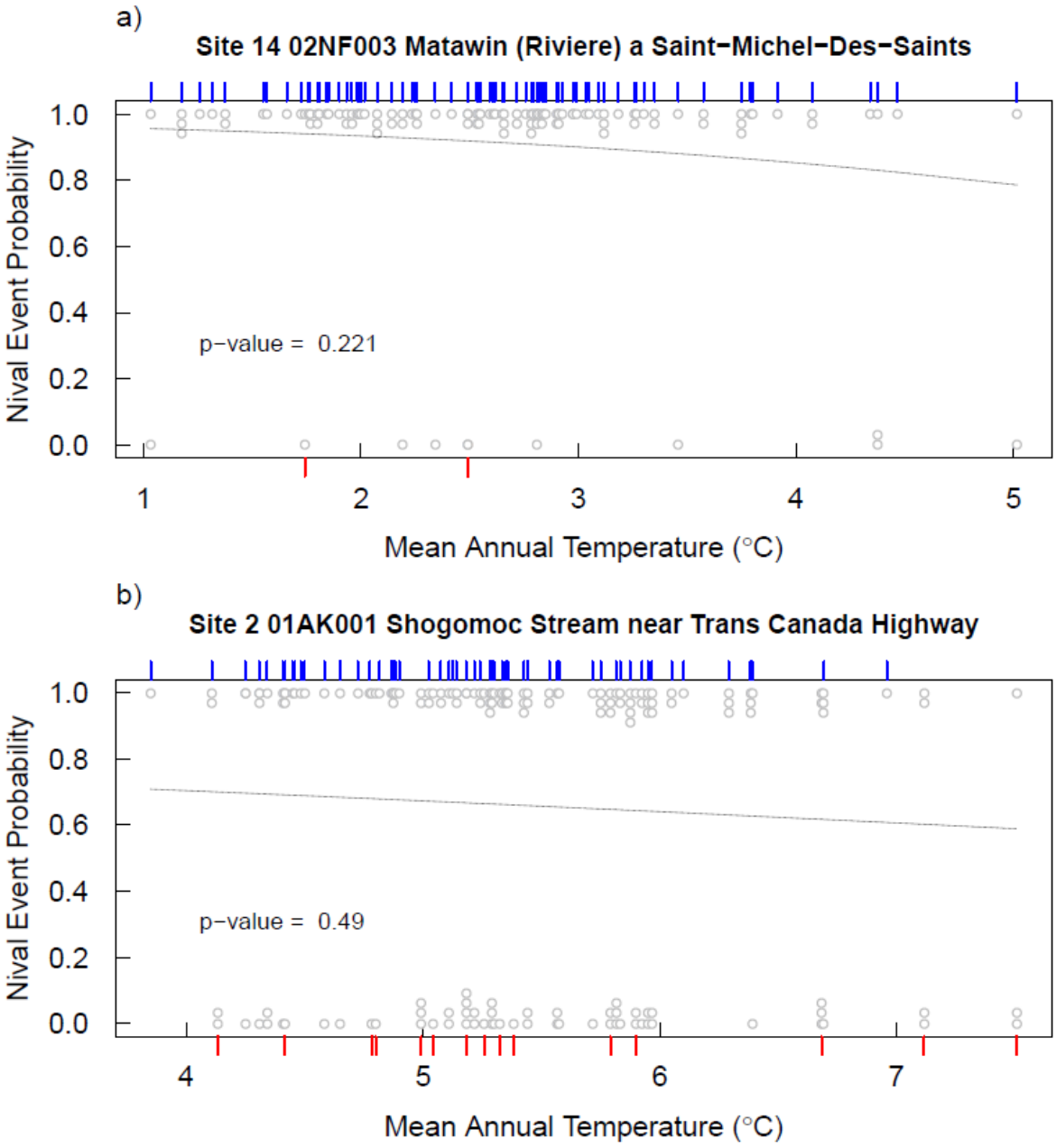
a)
Site 14 02NF003 Matawin (Riviere) a Saint−Michel−Des−Saints
Nival Event Probability
1.0
0.8
0.6
0.4
0.2
0.0
p−value = 0.221
1
2
3
4
5
Mean Annual Temperature (°C)
b)
Site 2 01AK001 Shogomoc Stream near Trans Canada Highway
Nival Event Probability
1.0
0.8
0.6
0.4
0.2
0.0
p−value = 0.49
4
5
6
7
Mean Annual Temperature (°C)

744

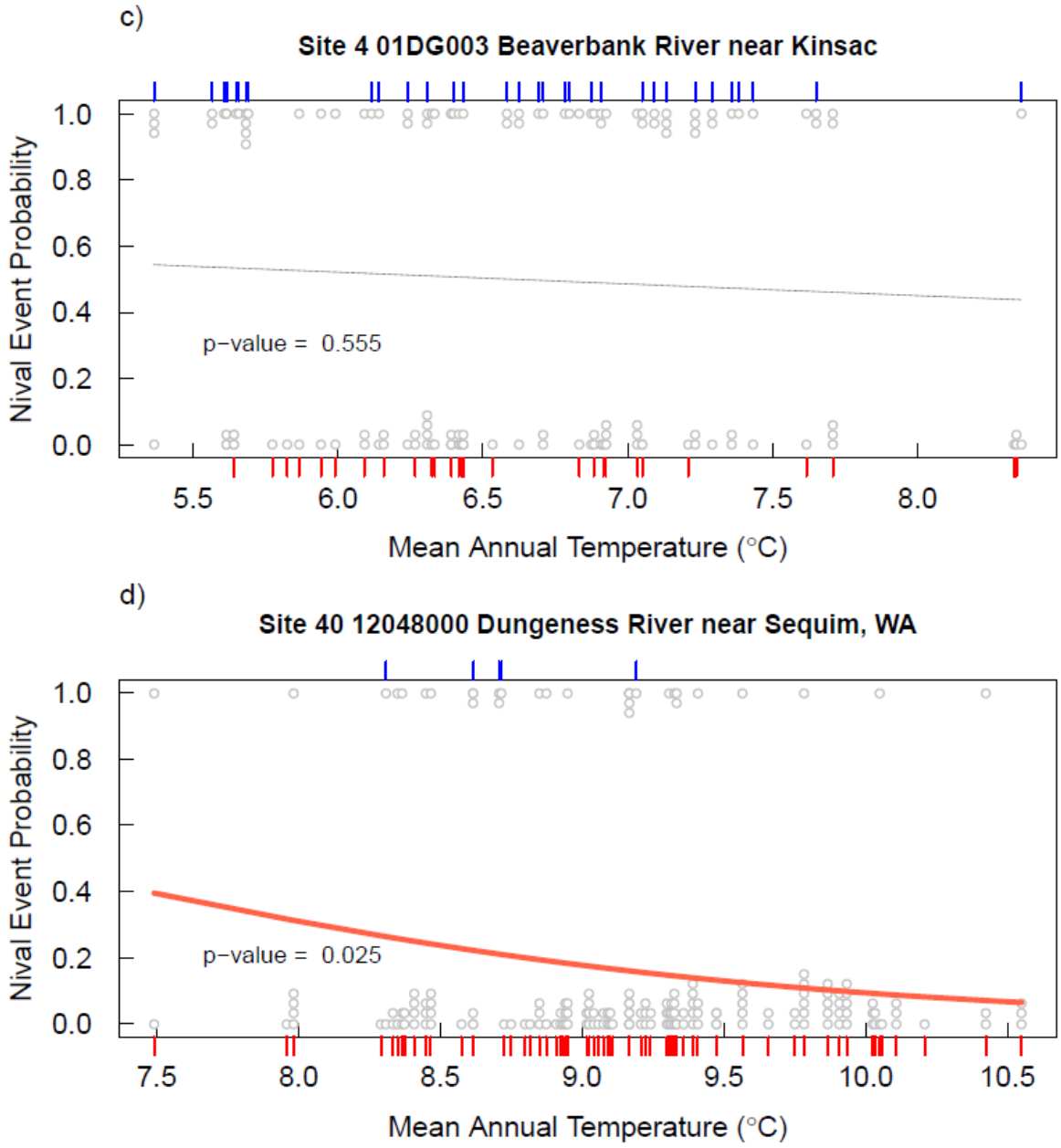

745

746 Figure 8 Time series of POT events and the results of the logistic regression based on annual
747 temperature. POT events are shown as gray circles either stacked at nival event probability of 1.0 (nival
748 events) or 0.0 (pluvial events). Annual maxima events are shown outside the frame as nival (blue, top),
749 or pluvial (red, bottom) tick marks. The line of the logistic regression is solid red if the p value is ≤ 0.05;
750 dashed red if the p value is > 0.05 but ≤ 0.10, and light gray otherwise. Figure S2 in the Supplementary
751 Material provides results for each of the 46 sites.

752

753

754

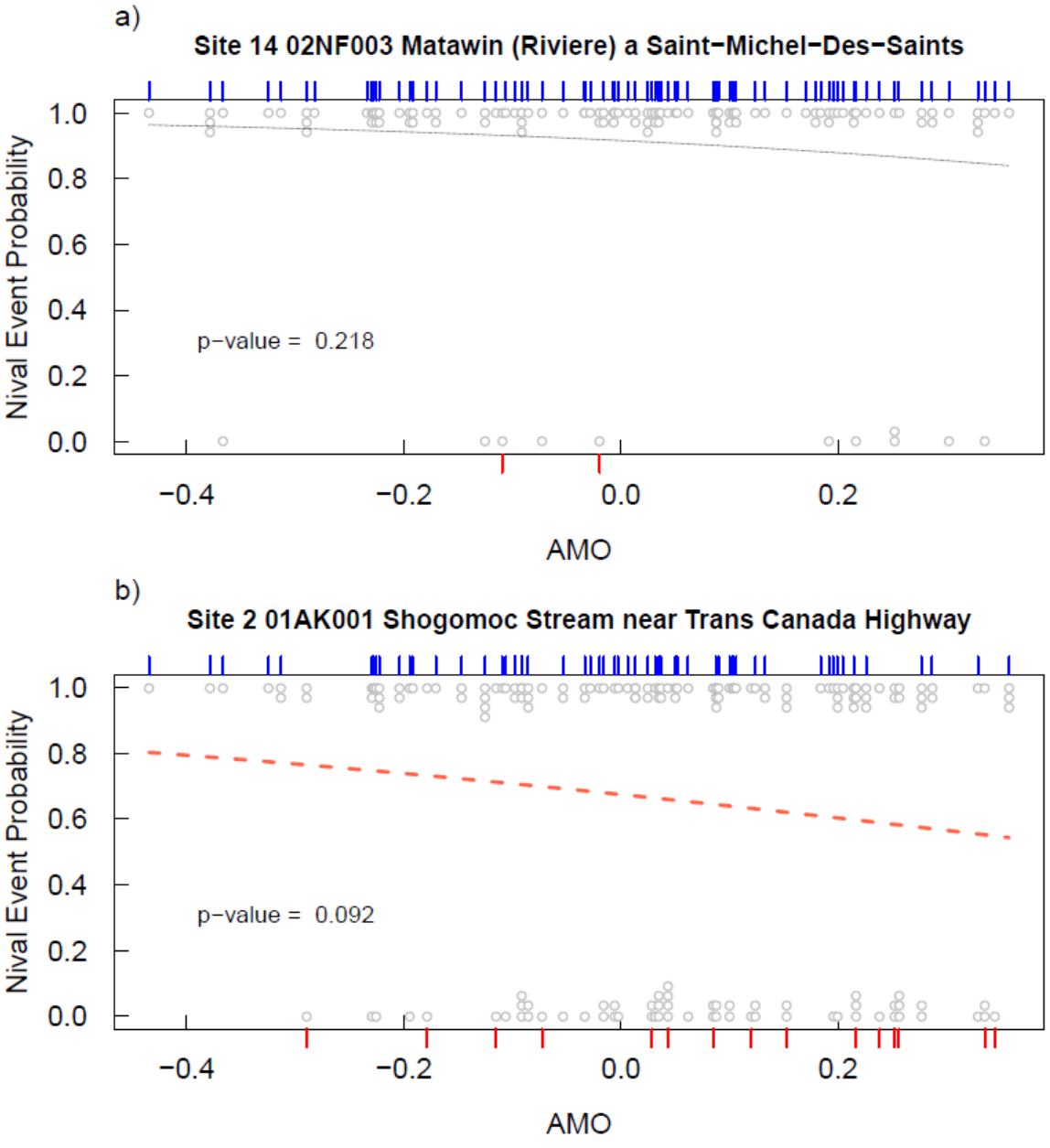
a)
Site 14 02NF003 Matawin (Riviere) a Saint−Michel−Des−Saints
Nival Event Probability
1.0
0.8
0.6
0.4
0.2
0.0
p−value = 0.218
−0.4
−0.2
0.0
0.2
AMO
b)
Site 2 01AK001 Shogomoc Stream near Trans Canada Highway
Nival Event Probability
1.0
0.8
0.6
0.4
0.2
0.0
p−value = 0.092
−0.4
−0.2
0.0
0.2
AMO

755

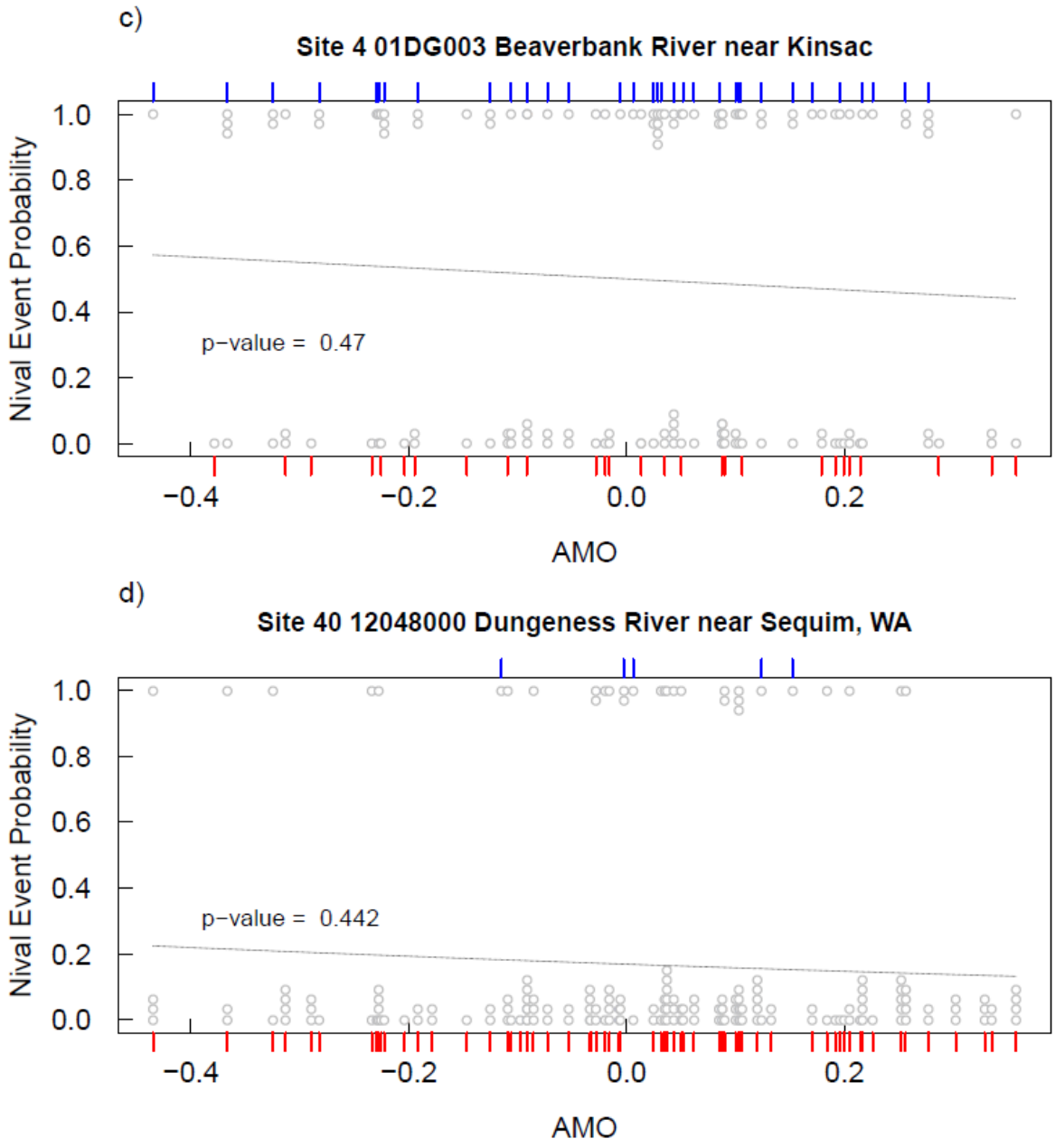

Figure 9 Time series of POT events and the results of the logistic regression based on AMO. POT events are shown as gray circles either stacked at nival event probability of 1.0 (nival events) or 0.0 (pluvial events). Annual maxima events are shown outside the frame as nival (blue, top), or pluvial (red, bottom) tick marks. The line of the logistic regression is solid red if the p value is ≤ 0.05; dashed red if the p value is > 0.05 but ≤ 0.10, and light gray otherwise.

Table 1 Station information for sites included in the analysis. The station names have been converted to the same case for consistency. Provinces and states are not included in station names in Canada unlike

764 most station names in the US. These are provided in a separate column and have not been removed

765 from station names for US stations.

Site	Station Number	Station Name	Prov. or State	Drainage Area (km^2)	Nival Fraction
1	01AD002	Saint John River at Fort Kent	ME/NB	14700	0.79
2	01AK001	Shogomoc Stream near Trans Canada Highway	NB	234	0.66
3	01AQ001	Lepreau River at Lepreau	NB	239	0.47
4	01DG003	Beaverbank River near Kinsac	NS	97	0.50
5	01EC001	Roseway River at Lower Ohio	NS	495	0.54
6	01EF001	Lahave River at West Northfield	NS	1250	0.54
7	01EO001	St. Marys River at Stillwater	NS	1350	0.48
8	01FB001	Northeast Margaree River at Margaree Valley	NS	368	0.54
9	01FB003	Southwest Margaree River near Upper Margaree	NS	357	0.50
10	02EA005	North Magnetawan River near Burk's Falls	ON	329	0.77
11	02EC002	Black River near Washago	ON	1510	0.70
12	02FC001	Saugeen River near Port Elgin	ON	3954	0.71
13	02KB001	Petawawa River near Petawawa	ON	4122	0.93
14	02NF003	Matawin (Riviere) a Saint-Michel-Des-Saints	QC	1390	0.91
15	02PJ007	Beaurivage (Riviere) a Sainte-Etienne	QC	709	0.68
16	02YL001	Upper Humber River near Reidville	NL	2110	0.66
17	04LJ001	Missinaibi River at Mattice	ON	8574	0.91
18	04NA001	Harricana (Riviere) 3.1 km en aval du Pont-Route 111	QC	3680	0.80
19	05AD005	Belly River near Mountain View	AB	319	0.97
20	05BB001	Bow River at Banff	AB	2210	1.00
21	05PB014	Turtle River near Mine Centre	ON	4768	0.75
22	08GA010	Capilano River above Intake	BC	173	0.00
23	08MG005	Lillooet River near Pemberton	BC	2100	0.77
24	01031500	Piscataquis River near Dover-Foxcroft	ME	769	0.62
25	01078000	Smith River near Bristol	NH	223	0.76
26	01144000	White River at West Hartford	VT	1790	0.72
27	01350000	Schoharie Creek at Prattsville NY	NY	613	0.56
28	01532000	Towanda Creek near Monroeton, PA	PA	554	0.56
29	03015500	Brokenstraw Creek at Youngsville, PA	PA	785	0.82
30	04056500	Manistique River near Manistique, MI	MI	2946	0.77
31	04124000	Manistee River near Sherman, MI	MI	2244	0.76
32	05120500	Wintering River nr Karlsruhe, ND	ND	1510	0.75
33	05131500	Little Fork River at Littlefork, MN	MN	4384	0.57
34	05291000	Whetstone River near Big Stone City, SD	SD	1047	0.54
35	05362000	Jump River at Sheldon, WI	WI	1477	0.74
36	06191500	Yellowstone River at Corwin Springs MT	MT	6784	1.00
37	06289000	Little Bighorn River at State Line nr Wyola MT	MT	471	1.00
38	06354000	Cannonball River at Breien, ND	ND	10598	0.57
39	12035000	Satsop River near Satsop, WA	WA	770	0.00
40	12048000	Dungeness River near Sequim, WA	WA	405	0.17
41	12175500	Thunder Creek near Newhalem, WA	WA	274	0.69
42	12186000	Sauk River Ab Whitechuck River near Darrington, WA	WA	398	0.36
43	12358500	Middle Fork Flathead River nr West Glacier MT	MT	2939	0.77

44	12414500	St Joe River at Calder ID	ID	2679	0.80
45	14020000	Umatilla River above Meacham Creek, nr Gibbon, OR	OR	341	0.55
46	15072000	Fish C nr Ketchikan AK	AK	91	0.00

766

767

768 Table 2 Number of stations in each change status category for temporal, annual temperature and climate index logistic regression analysis. The

769 "-1" indicates the climate index for the preceding year. The six sites with no change are the three with only nival and three with only pluvial

770 events and hence the nival fraction is always 1 or always 0, and does not change.

Change Status	Temporal	Annual Temp.	AMO	AMO-1	NAO	NAO-1	PDO	PDO-1	SOI	SOI-1
Inc 5%	0	1	1	0	0	1	1	2	0	1
Inc 10%	0	0	0	3	0	1	1	3	1	1
Inc N.S.	5	9	16	16	17	14	14	20	14	20
No Change	6	6	6	6	6	6	6	6	6	6
Dec N.S.	26	21	19	20	22	21	21	15	20	15
Dec 10%	2	2	3	1	0	1	2	0	2	1
Dec 5%	7	7	1	0	1	2	1	0	3	2

771

772